PLoS one

A Novel Screening System for Claudin Binder Using Baculoviral Display

Hideki Kakutani[1☯], Azusa Takahashi[1☯], Masuo Kondoh[1*], Yumiko Saito[1], Toshiaki Yamaura[1], Toshiko Sakihama[2], Takao Hamakubo[2], Kiyohito Yagi[1*]

1 Laboratory of Bio-Functional Molecular Chemistry, Graduate School of Pharmaceutical Sciences, Osaka University, Suita, Osaka, Japan, 2 Department of Molecular Biology and Medicine, Research Center for Advanced Science and Technology, The University of Tokyo, Meguro, Tokyo, Japan

Abstract

Recent progress in cell biology has provided new insight into the claudin (CL) family of integral membrane proteins, which contains more than 20 members, as a target for pharmaceutical therapy. Few ligands for CL have been identified because it is difficult to prepare CL in an intact form. In the present study, we developed a method to screen for CL binders by using the budded baculovirus (BV) display system. CL4-displaying BV interacted with a CL4 binder, the C-terminal fragment of *Clostridium perfringens* enterotoxin (C-CPE), but it did not interact with C-CPE that was mutated in its CL4-binding region. C-CPE did not interact with BV and CL1-displaying BV. We used CL4-displaying BV to select CL4-binding phage in a mixture of a scFv-phage and C-CPE-phage. The percentage of C-CPE-phage in the phage mixture increased from 16.7% before selection to 92% after selection, indicating that CL-displaying BV may be useful for the selection of CL binders. We prepared a C-CPE phage library by mutating the functional amino acids. We screened the library for CL4 binders by affinity to CL4-displaying BV, and we found that the novel CL4 binders modulated the tight-junction barrier. These findings indicate that the CL-displaying BV system may be a promising method to produce a novel CL binder and modulator.

Citation: Kakutani H, Takahashi A, Kondoh M, Saito Y, Yamaura T, et al. (2011) A Novel Screening System for Claudin Binder Using Baculoviral Display. PLoS ONE 6(2): e16611. doi:10.1371/journal.pone.0016611

Editor: Vladimir Uversky, University of South Florida College of Medicine, United States of America

Received November 22, 2010; **Accepted** December 24, 2010; **Published** February 14, 2011

Funding: This work was supported by a Grant-in-Aid for Scientific Research from the Ministry of Education, Culture, Sports, Science and Technology, Japan (21689006), by a Health and Labor Sciences Research Grant from the Ministry of Health, Labor and Welfare of Japan, by Takeda Science Foundation, by a Suzuken Memorial Foundation, by a grant from Kansai Biomedical Cluster project in Saito, which is promoted by the Knowledge Cluster Initiative of the Ministry of Education, Culture, Sports, Science and Technology, Japan and by a Research Grant for Promoting Technological Seeds from Japan Science and Technology Agency. A.T. is supported by Research Fellowships of the Japan Society for the Promotion of Science for Young Scientists. The funders had no role in study design, data collection and analysis, decision to publish, or preparation of the manuscript.

Competing Interests: The authors have declared that no competing interests exist.

* E-mail: masuo@phs.osaka-u.ac.jp (MK); yagi@phs.osaka-u.ac.jp (KY)

☯ These authors contributed equally to this work.

Introduction

Tight junctions (TJ) are intercellular adhesion complexes in epithelial and endothelial cells; TJs are located in the most apical part of the complexes [1]. TJs have a barrier function and a fence function [2–4]. TJs contribute to epithelial and endothelial barrier functions by restricting the diffusion of solutes through the paracellular pathway. TJs maintain cellular polarity by preventing the free movement of membrane proteins between the apical and basal membranes [5]. Loss of cell-cell adhesion and cellular polarity commonly occurs in the early stages of cancer [6]. Modulation of the TJ barrier function can be a method to enhance drug absorption, and TJ components exposed on the surface of cancer cells can be a target for cancer therapy.

Biochemical analyses of TJs have identified TJ components, such as occludin, claudins (CLs) and junction adhesion molecule [7]. The CL family contains more than 20 integral tetra-transmembrane proteins that play pivotal roles in the TJ barrier and fence functions. CL1-deficient mice lack the epidermal barrier, while CL5-deficient mice lack the blood-brain barrier [8,9], indicating that the regulation of the TJ barrier by modulation of CLs may be a promising method for drug delivery. *Clostridium perfringens* enterotoxin (CPE) causes food poisoning in humans [10]. An interaction between the C-terminal domain of CPE (C-CPE) with CL4 deregulates the TJ barrier [11,12]. We previously found that C-CPE enhances jejunal absorption through its interaction with CL4, indicating that a CL binder is a potent drug-delivery system [13].

The majority of lethal cancers are derived from epithelial tissues [14]. Malignant tumor cells frequently exhibit abnormal TJ function, followed by the deregulation of cellular polarity and intercellular contact, which is commonly observed in both advanced tumors and the early stages of carcinogenesis [6]. Some CLs are overexpressed in various types of cancers. For example, CL3 and CL4 are overexpressed in breast, prostate, ovarian, pancreatic and gastric cancers. CL1, CL7, CL10 and CL16 are overexpressed in colon, gastric, thyroid and ovarian cancers, respectively [15,16]. These findings indicate that the CLs may be a target molecule for cancer therapy. A receptor for CPE is CL4 [11,12]. CPE has anti-tumor activity against human pancreatic and ovarian cancers without side effects [17,18]. The CLs binders will be useful for cancer-targeting therapy.

As above, recent investigations of CLs provide new insight into their use as pharmaceutical agents; for example, a CL binder may be used in drug delivery and anti-tumor therapy. Selection of a CL binder by using a recombinant CL protein is a putative method to

prepare a CL binder. However, CLs are four-transmembrane proteins with high hydrophobicity; there has been little success in the preparation of intact CL protein. Recently, a novel type of protein expression system that uses baculovirus has been developed. Membrane proteins are displayed on the budded baculovirus (BV) in their active form [19–21], indicating that the BV system may be useful for the preparation of a CL binder. In the present study, we investigated whether a CL binder was screened by using a CL-displaying BV.

Results

Preparation of CL4-displaying BV

C-CPE is the only known CL binder and modulator [12,13,22]. C-CPE has affinity to CL4 in a nanomolar range [23]. We chose C-CPE and CL4 as models of the CL binder and CL, respectively. Several reports indicate that membrane proteins expressed on the surface of BV are in an intact form [19–21]. To check the expression of CL4 on the BV, we performed immunoblot analysis of the lysate of CL4-BV against CL4. As shown in Fig. 1A, CL4 was detected in the virus lysates. To determine if the CL4 expressed on the virus has an intact form, we performed enzyme-linked immunosorbent assay (ELISA) with CL4-BV-coated immunoplates. C-CPE binds to the extracellular loop domain of CL4 [23]. After the addition of C-CPE to the CL4-BV-coated plate, the C-CPE bound to the CL4-BV-coated plate was detected by anti-his-tag antibody, followed by incubation with horseradish peroxidase-labeled antibody. C-CPE was dose-dependently bound to CL4-BV, whereas C-CPE did not interact with wild-BV (Fig. 1B). Deletion of the CL4-binding region (C-CPE303) attenuated the interaction of C-CPE with CL4-BV (Fig. 1C). Together, these results indicate that the CL4 displayed on BV may have an intact extracellular loop region.

Selection of C-CPE-phage by using CL4-BV

We next examined the interaction between C-CPE-phage and CL4-BV. As shown in Fig. 2A, C-CPE-phage bound to CL4-BV but not to wild-BV, and a scFv-phage did not bind to CL4-BV. To determine if CL-BV can be used to select CL binders, we prepared a mixture of C-CPE-phage and scFv-phage at a ratio of 2:10 and used CL4-BV to select CL4-binding phage in the mixtures. The amount of C-CPE-phage was increased to 11 of 12 clones in the mixture (Fig. 2B), indicating that CL-BV may be useful in the preparation of CL binders.

We previously found that each substitution of S304, S305, S307, N309, S313 and K318 with alanine increased the binding of C-CPE to CL4 [24]. Here, we prepared a phage library for C-CPE by randomly changing the functional 6 amino acids to any of the 20 amino acids. To confirm the diversity of the library, we checked the sequences of 17 randomly isolated clones. Each of the 17 clones had a different sequence, indicating that the library has a diverse population of C-CPE mutants (Table 1).

Then, we screened the CL4-binding phage by their affinity to CL4-BV. After addition of the C-CPE library to CL4-BV-adsorbed tubes, the CL4-BV-bound phages were recovered (1st screening). We repeated this screening process two more times (2nd screening and 3rd screening). If the number of CL4-bound phage is increased during the screening, the ratio of the incubated phage titers to the recovered phage titers will increase. As shown in Fig. 3A, the ratio was increased during screening from 4.5×10^{-7} to 5.5×10^{-5}, indicating that the screening system for CL4 binders may work. Indeed, the number of monoclonal phage clones with high affinity to CL4-BV was increased after the 3rd screening compared with that after the 2nd screening (Fig. 3B).

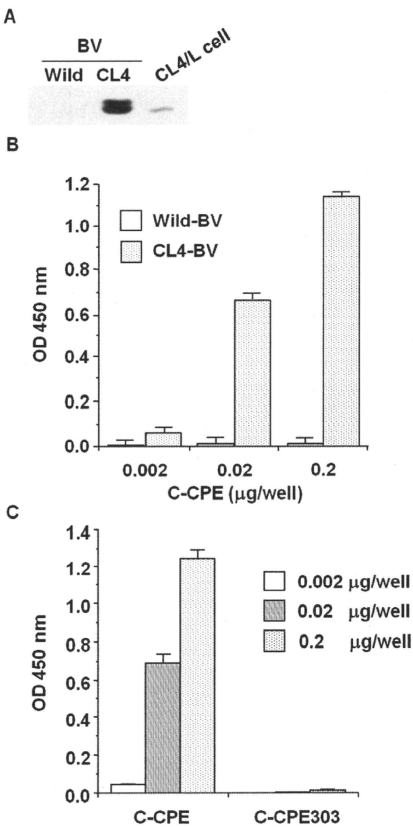

Figure 1. Preparation of CL4-displaying BV. A) Immunoblot analysis. Wild-BV and CL4-BV (0.1 μg/lane) were subjected to SDS-PAGE, followed by immunoblot analysis with anti-CL4 antibody. The lysate of CL4-expressing L (CL4/L) cells was used as a positive control. B, C) Interaction of a CL4 binder with CL4-BV. Immunotubes were coated with the wild-BV or CL4-BV, and C-CPE (B) or mutated C-CPE (C) was added to the BV-coated immunotubes at the indicated concentration. C-CPE bound to the BV-coated tubes was detected by ELISA with an anti-his-tag antibody.
doi:10.1371/journal.pone.0016611.g001

We analyzed the sequences of the CL4-BV-bound phages and got novel CL4-binder candidates with amino acid sequences that differed from the wild-type sequence (Table 2). To investigate their CL4-binding, we prepared the recombinant proteins of the binders and investigated their interaction with CL4 by ELISA with CL-BVs. As shown in Fig. 4A, the novel C-CPE derivatives had affinity to CL4 but not CL1. Next, we investigated whether the novel CL4 binders modulate TJ barrier in Caco-2 monolayer cell sheets, a popular model for the evaluation of TJ barriers [25].

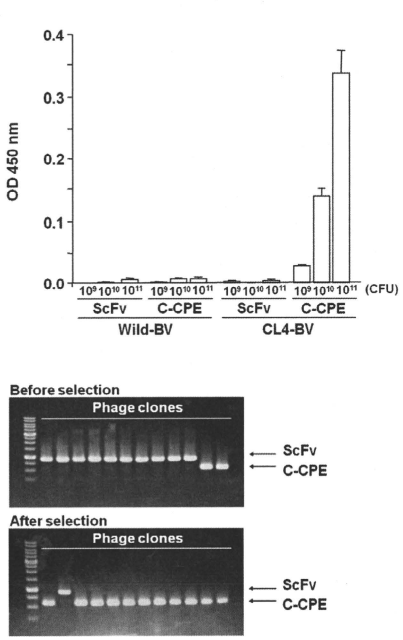

Figure 2. Selection of C-CPE-displaying phage by using the CL4-BV system. A) Interaction of C-CPE-displaying phage with CL4-BV. Wild-BV or CL4-BV was coated on an immunoplate, and then scFv-displaying phage or C-CPE-displaying phage was added to the BV-coated immunoplate at the indicated concentrations. The BV-bound phages were detected by ELISA with anti-M13 antibody as described in Materials and methods. Data are representative of two independent experiments. Data are means ± SD (n = 3). B) Enrichment of C-CPE-displaying phage by the BV system. A mixture of scFv-phage and C-CPE-phage (mixing ratio of scFv-phage to C-CPE-phage = 2:10) was incubated with a CL4-BV-coated immunotube, and the bound phages were recovered. Each phage clone was identified by PCR amplification, followed by agarose gel electrophoresis. Upper and lower pictures are before and after the selection, respectively. The putative sizes of the PCR products are 856 and 523 bp in scFv and C-CPE, respectively. The data are representative of two independent experiments.
doi:10.1371/journal.pone.0016611.g002

Treatment of the cells with C-CPE resulted in decreased transepithelial electrical resistance (TEER) values, a marker of TJ integrity, and the TEER values increased after removal of C-CPE. The C-CPE derivatives (clones 1–5) had TJ-modulating activity similar to that of C-CPE (Fig. 4B).

Discussion

CL is a promising target for pharmaceutical therapy. However, CL has low antigenicity, and there has been little success in the preparation of monoclonal antibody against the extracellular loop region of CL. The three-dimensional structure of CL has never been determined, so it is impossible to perform a theoretical design of a CL binder based on the structural information. In the present study, we developed a novel screening system for CL binders by using a BV system and a C-CPE phage display library, and we used this system to identify novel CL4 binders.

Table 1. C-CPE phage library.

	304	305	307	309	313	318
C-CPE	**S**	**S**	**S**	**N**	**S**	**K**
Clone 1	V	T	C	V	N	K
2	C	P	A	H	L	T
3	A	G	G	V	P	P
4	R	G	H	L	E	H
5	A	A	P	S	R	Q
6	P	A	P	D	P	A
7	C	T	T	T	N	K
8	H	P	S	P	G	H
9	R	G	G	R	N	R
10	A	P	S	T	Q	P
11	V	L	G	N	M	R
12	P	P	A	T	F	R
13	G	D	C	S	N	L
14	F	R	V	F	R	N
15	S	Q	Q	W	T	T
16	S	R	L	E	W	Q
17	K	R	E	R	Q	S

Phage clones were randomly picked up from the C-CPE phage library, and the amino acids sequences of C-CPE mutant were analyzed.
doi:10.1371/journal.pone.0016611.t001

In ligand screening, the preparation of a receptor for the ligand is very critical. Membrane proteins are especially difficult to prepare as recombinant protein with an intact structure. Functional membrane proteins such as cell-surface proteins are heterologously expressed on BV in their native forms [19–21]. Interactions between membrane proteins can be detected by using receptor-displaying and ligand-displaying BV [21]. In the present report, we found that CL4-BV interacts with a CL4 binder, C-CPE, but it does not interact with C-CPE303 that lacks the CL4-binding residues of C-CPE. The CL4-binding site of C-CPE corresponds to that of CPE; so, the second extracellular loop of CL appears to be the C-CPE-binding site [23,26]. These findings indicate that CL4 displayed on BV may have native form. We anticipate that CL-BV will be useful for the preparation of CL binders, such as peptides and antibodies.

To the best of our knowledge, the preparation of CL binder has been performed by only four groups. Offner et al. prepared polyclonal antibodies against extracellular domains of CL3 and CL4 [27], Ling et al. screened peptide types of CL4 binder by using a 12-mer peptide phage display library and CL4-expressing cells [28], Suzuki et al. generated a monoclonal antibody against the second extracellular loop of CL4 from mice immunized with a human pancreatic cancer cell line [29] and Romani et al. screened scFv against CL3 by using a human antibody phage display library [30]. However, the CL modulators have never been developed; thus, C-CPE is the only known CL4 modulator [12]. In the present study, we prepared a C-CPE phage library containing C-CPE mutants in which each of the 6 functional amino acids was randomly replaced with an amino acid, and we isolated CL4 binders by using CL4-BV as a screening ligand. Interestingly, all of

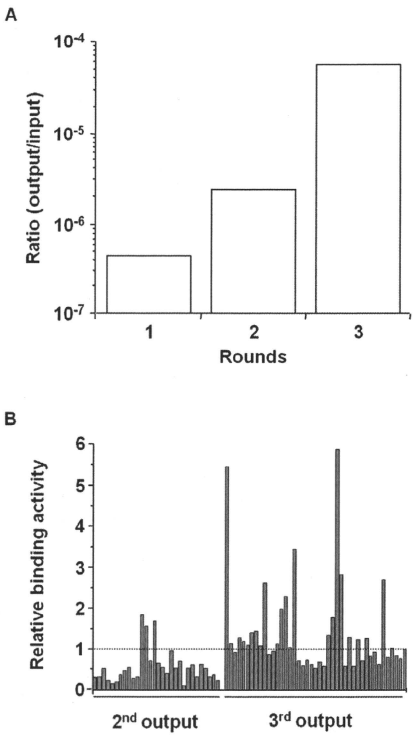

Figure 3. Screening of a novel CL4 binder. A) Enrichment of phages with affinity to CL4-BV. CL4-BVs coated on immunotubes were incubated with the C-CPE-derivative phage library at 1.6×10^{12} CFU titer (1st input phage). The phages bound to CL4-BV were recovered (1st output phage). The CL4-BV-binding phages were subjected to two additional cycles of the incubation and wash step, resulting in 2nd, 3rd output phage. The ratio of output phage to input phage titers was calculated. B) Monoclonal analysis of C-CPE-derivative phage. CL4-BV-bound phage clones were isolated from the 2nd and 3rd output phages, and the interaction of the monoclonal phage with CL4-BV was examined by ELISA with anti-M13 antibody as described in Materials and methods. Data are expressed as relative binding to that of C-CPE-phage indicated by the most right column.
doi:10.1371/journal.pone.0016611.g003

the CL4 binders modulated TJ barriers. We are investigating why the substitution of the amino acids with the other amino acids modulated CL4. These findings indicate that a BV screening system with a C-CPE library may be a powerful method to develop CL modulators.

The CL family forms various types of TJ barriers through combinations of its more than 20 members in homophilic/heterophilic CL strands [31,32]. Intercellular proteins ZO-1 and ZO-2 determine the localization of CL strands [33]. If a screening system to reconstitute heterogeneous CL strands with ZO-1 and/or ZO-2 is developed, then useful and effective CL modulators can be identified. In this point, the BV system has extremely superior features. G protein and G protein-coupled receptors have been

Table 2. CL4-binding phages.

	304	305	307	309	313	318
C-CPE	**S**	**S**	**S**	**N**	**S**	**K**
Clone 1	R	V	S	A	R	R
2	R	S	V	A	R	K
3	G	D	G	R	T	R
4	S	A	P	R	S	A
5	R	S	L	K	S	K

The sequences of C-CPE mutant in the CL4-binding phages were analyzed.
doi:10.1371/journal.pone.0016611.t002

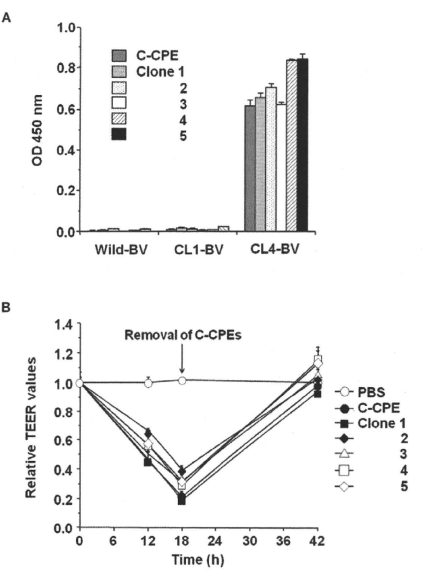

Figure 4. Isolation of a novel CL4 modulator. A) Interaction of the C-CPE derivatives with CL4. C-CPE derivatives were prepared as his-tagged recombinant proteins. The C-CPE derivatives (0.02 μg) were added to CL-BV-coated immunoplates, followed by detection of the C-CPE derivatives bound to CL-BV. Data are means ± SD (n = 4). B) Modulation of tight junction-barriers. Caco-2 cells were cultured on Transwell™ chambers. When TEER values reach a plateau, the cells were treated with C-CPE or C-CPE derivatives at the indicated concentrations. After 18 h of exposure to the C-CPEs, the cells were washed with medium to remove C-CPEs, and then the cells were cultured for an additional 24 h. Changes in TEER values were monitored during the C-CPEs treatment. Relative TEER values were calculated as the ratio of TEER values at 0 h. Data are representative of two independent experiments. The data are means ± SD (n = 4).
doi:10.1371/journal.pone.0016611.g004

functionally reconstituted in BV [20,34], and functional γ-secretase complexes have also been reconstituted on BV [35]. In the near future, the reconstituted CL system on BV will be developed and used for the screening of CL binders and modulators, hopefully leading to breakthroughs in pharmaceutical therapies that target CLs.

Materials and Methods

Recombinant BV construction and Sf9 cell culture

Recombinant BV was prepared by using the Bac-to-Bac expression system, according to the manufacturer's instructions (Invitrogen, Gaithersburg, MD). Briefly, mouse CL1 and CL4 cDNA (kind gifts from Dr. M Furuse, Kobe University, Japan) were inserted into pFastBac1, and the resulting plasmids were transduced into DH10Bac *E. Coli* cells. Recombinant bacmid DNA was extracted from the cells. Sf9 cells were transduced with the bacmid coding CL, and the recombinant BV was recovered by centrifugation of the conditioned medium [36].

Preparation of the BV fractions

Sf9 cells (2×10^6 cells) were infected with recombinant BV at a multiplicity of infection of 5. Seventy-two hours after infection, the BV fraction was recovered from the culture supernatant of infected Sf9 cells by centrifugation. The pellets of the BV fraction were resuspended in Tris-buffered saline (TBS) containing 1% protease inhibitor cocktail (Sigma-Aldrich, St. Louis, MO) and then stored at 4°C until use. The expression of CL1 and CL4 in the BV was confirmed by sodium dodecyl sulfate-polyacrylamide gel electrophoresis (SDS-PAGE) and immunoblot analysis with anti-CL antibodies (Zymed Laboratory, South San Francisco, CA).

Preparation of mutant C-CPE library

C-CPE fragments in which the functional amino acids (S304, S305, S307, N309, S313 and K318) [24] were randomly mutated were prepared by polymerase chain reaction (PCR) with pET-H_{10}PER as a template, a forward primer (5′-catgccatggccgatatagaaaaagaaatccttgatt-tagctgctg-3′, Nco I site is underlined) and a reverse primer (5′-ttttccttttgcggccgcaaa*nnn*ttgaaataatat*nnn*ataagggta*nnn*tcc*nnn*ata*nnn*nnat-tagcttt-3′, Not I site is underlined, and the randomly mutated amino acids are in italics). The PCR fragments were inserted into a pY03 phagemid at the NcoI/NotI sites [22]. The resultant phagemid containing the C-CPE mutant library was transduced into *E. coli* TG1 cells, and then the cells were stored at −80°C.

Preparation of phage

TG1 cells containing phagemid coding a scFv, C-CPE, C-CPE mutant or C-CPE mutant library were culture in 2YT medium containing 2% glucose and ampicillin. When the cells grew to a growing phage, M13K07 helper phages (Invitrogen) were added, and the medium was changed into 2YT medium containing ampicillin and kanamycin. After an additional 6 h of culture, the phages in the conditioned medium were precipitated with polyethylene glycol. The phages were suspended in phosphate-buffered saline (PBS) and stored at 4°C until use.

ELISA

Wild-BVs or CL-BVs (0.5 μg/well) were adsorbed onto an immunoplate (Greiner Bio-One, Frickenhausen, Germany). The wells were washed with PBS and blocked with TBS containing 1.6% BlockAce (Dainippon Sumitomo Pharma, Osaka, Japan). C-CPEs or phages were incubated in the immunoplate, and the BV-bound C-CPEs or phages were detected by using anti-his-tag antibody (Novagen, Darmstadt, Germany) or anti-M13 antibody (Amersham-Pharmacia Biotech, Uppsala, Sweden), respectively, horseradish peroxidase-labelled secondary antibody and TMB peroxidase substrate (Nacalai Tesque, Kyoto, Japan). The immunoreactive C-CPEs or phages were quantified by the measurement of absorbance at 450 nm. In the screening of phages, the data were normalized by the amounts of phages, which were quantified by ELISA for the FLAG-tag contained in the coat protein.

Selection of phage by using BV

A total of 0.5 μg of BV was adsorbed onto an immunotube (Nunc, Roskilde, Denmark). The tube was washed with PBS and blocked with TBS containing 4.0% BlockAce. The BV-coated tubes were incubated with mixture of phages, and then the tubes were washed 15 times with PBS and 15 times with PBS containing 0.05% Tween 20. The phages bound to the tube were eluted with 100 mM HCl. TG1 cells were infected with the eluted phages, and phages were prepared as described above. The resulting phages were subjected to repeated selection by using the BV-coated immunotubes.

Identification of a phage clone

To identify an isolated phage clone, we performed PCR or sequencing analysis. We amplified the inserted fragment into the phagemid by PCR using forward primer 5′-caggaaacagctatgac-3′ and reverse primer 5′-gtaaatgaattttctgtatgagg-3′. The resultant PCR products were subjected to agarose gel electrophoresis followed by staining with ethidium bromide. We performed a sequence analysis with primer 5′-gtaaatgaattttctgtatgagg-3′.

Measurement of phage titer

To quantify the concentration of phages, we measured the titer (colony formation unit (CFU)/ml) of the phage solution. Briefly, the phage solution was diluted to 10^{-5}–10^{-10} with PBS. The diluted solution was seeded onto Petrifilm™ (Tech-Jam, Osaka, Japan). After 24 h of incubation, the colonies were counted, and the titer was calculated.

Purification of C-CPE mutants

C-CPE and C-CPE303, in which the CL-4 binding region of C-CPE was deleted, were prepared as described previously [13]. To prepare plasmid containing C-CPE mutants, the C-CPE mutant fragment was PCR-amplified by using phagemids coding C-CPE mutants as a template. The resulting PCR fragment was inserted into pET16b, and the sequence was confirmed. The plasmids were transduced into *E. coli* strain BL21 (DE3), and production of mutant C-CPEs was induced by the addition of isopropyl-D-thiogalactopyranoside. The harvested cells were lysed in buffer A (10 mM Tris-HCl, pH 8.0, 400 mM NaCl, 5 mM $MgCl_2$, 0.1 mM phenylmethanesulfonyl fluoride, 1 mM 2-mercaptoethanol, and 10% glycerol) that was supplemented with 8 M urea when necessary. The lysates were applied to HiTrap™ Chelating HP (GE Healthcare, Buckinghamshire, UK), and mutant C-CPEs were eluted with buffer A containing 100–400 mM imidazole. The buffer was exchanged with PBS by using a PD-10 column (GE Healthcare), and the purified protein was stored at −80°C until use. Purification of the mutant C-CPEs was confirmed by SDS-PAGE, followed by staining with Coomassie Brilliant Blue and by immunoblotting with anti-his-tag antibody (Novagen). Protein was quantified by using a BCA protein assay kit with bovine serum albumin as a standard (Pierce Chemical, Rockford, IL).

TEER assay

Caco-2 cells were seeded in Transwell™ chambers (Corning, NY) at a subconfluent density. The TEER of the Caco-2 monolayer cell sheets on the chamber was monitored by using a Millicell-ERS epithelial volt-ohmmeter (Millipore, Billerica, MA). When TEER values reached a plateau, indicating that TJs were well-developed in the cell sheets, the Caco-2 monolayers were treated with C-CPE or C-CPE mutants on the basal side of the chamber. Changes in TEER values were monitored. The TEER values were normalized by the area of the Caco-2 monolayer, and the TEER value of a blank Transwell™ chamber (background) was subtracted.

Acknowledgments

We thank Drs. S. Tsunoda (National Institute of Biomedical Innovation, Japan), Y. Tsutsumi, Y. Mukai (Osaka University, Japan) for their kind instruction of phage display technology. We also thank Drs. Y. Horiguchi (Osaka University, Japan), S. Tsukita (Kyoto University, Japan) and members of our laboratory for providing us C-CPE cDNA, CL-expressing cells and their useful comments and discussion, respectively.

Author Contributions

Conceived and designed the experiments: MK TS TH KY. Performed the experiments: HK AT MK YS TY TS. Analyzed the data: HK AT MK KY. Contributed reagents/materials/analysis tools: HK AK TS TH. Wrote the manuscript: HK MK TY.

References

1. Farquhar MG, Palade GE (1963) Junctional complexes in various epithelia. J Cell Biol 17: 375–412.
2. Anderson JM, Van Itallie CM, Fanning AS (2004) Setting up a selective barrier at the apical junction complex. Curr Opin Cell Biol 16: 140–145.
3. Balda MS, Matter K (1998) Tight junctions. J Cell Sci 111(Pt 5): 541–547.
4. Tsukita S, Furuse M, Itoh M (2001) Multifunctional strands in tight junctions. Nat Rev Mol Cell Biol 2: 285–293.
5. Mitic LL, Anderson JM (1998) Molecular architecture of tight junctions. Annu Rev Physiol 60: 121–142.
6. Wodarz A, Nathke I (2007) Cell polarity in development and cancer. Nat Cell Biol 9: 1016–1024.
7. Schneeberger EE, Lynch RD (2004) The tight junction: a multifunctional complex. Am J Physiol 286: C1213–C1228.
8. Furuse M, Hata M, Furuse K, Yoshida Y, Haratake A, et al. (2002) Claudin-based tight junctions are crucial for the mammalian epidermal barrier: a lesson from claudin-1-deficient mice. J Cell Biol 156: 1099–1111.
9. Nitta T, Hata M, Gotoh S, Seo Y, Sasaki H, et al. (2003) Size-selective loosening of the blood-brain barrier in claudin-5-deficient mice. J Cell Biol 161: 653–660.
10. McClane BA (1994) *Clostridium perfringens* enterotoxin acts by producing small molecule permeability alterations in plasma membranes. Toxicology 87: 43–67.
11. Katahira J, Inoue N, Horiguchi Y, Matsuda M, Sugimoto N (1997) Molecular cloning and functional characterization of the receptor for *Clostridium perfringens* enterotoxin. J Cell Biol 136: 1239–1247.
12. Sonoda N, Furuse M, Sasaki H, Yonemura S, Katahira J, et al. (1999) *Clostridium perfringens* enterotoxin fragment removes specific claudins from tight junction strands: Evidence for direct involvement of claudins in tight junction barrier. J Cell Biol 147: 195–204.
13. Kondoh M, Masuyama A, Takahashi A, Asano N, Mizuguchi H, et al. (2005) A novel strategy for the enhancement of drug absorption using a claudin modulator. Mol Pharmacol 67: 749–756.
14. Jemal A, Siegel R, Ward E, Hao Y, Xu J, et al. (2008) Cancer statistics, 2008. CA Cancer J Clin 58: 71–96.
15. Kominsky SL (2006) Claudins: emerging targets for cancer therapy. Expert Rev Mol Med 8: 1–11.
16. Morin PJ (2005) Claudin proteins in human cancer: promising new targets for diagnosis and therapy. Cancer Res 65: 9603–9606.
17. Michl P, Buchholz M, Rolke M, Kunsch S, Lohr M, et al. (2001) Claudin-4: a new target for pancreatic cancer treatment using *Clostridium perfringens* enterotoxin. Gastroenterology 121: 678–684.
18. Santin AD, Cane S, Bellone S, Palmieri M, Siegel ER, et al. (2005) Treatment of chemotherapy-resistant human ovarian cancer xenografts in C.B-17/SCID mice by intraperitoneal administration of *Clostridium perfringens* enterotoxin. Cancer Res 65: 4334–4342.
19. Loisel TP, Ansanay H, St-Onge S, Gay B, Boulanger P, et al. (1997) Recovery of homogeneous and functional beta 2-adrenergic receptors from extracellular baculovirus particles. Nat Biotechnol 15: 1300–1304.
20. Sakihama T, Masuda K, Sato T, Doi T, Kodama T, et al. (2008) Functional reconstitution of G-protein-coupled receptor-mediated adenylyl cyclase activation by a baculoviral co-display system. J Biotechnol 135: 28–33.
21. Sakihama T, Sato T, Iwanari H, Kitamura T, Sakaguchi S, et al. (2008) A simple detection method for low-affinity membrane protein interactions by baculoviral display. PLoS ONE 3: e4024.
22. Ebihara C, Kondoh M, Hasuike N, Harada M, Mizuguchi H, et al. (2006) Preparation of a claudin-targeting molecule using a C-terminal fragment of *Clostridium perfringens* enterotoxin. J Pharmacol Exp Ther 316: 255–260.
23. Fujita K, Katahira J, Horiguchi Y, Sonoda N, Furuse M, et al. (2000) *Clostridium perfringens* enterotoxin binds to the second extracellular loop of claudin-3, a tight junction integral membrane protein. FEBS Lett 476: 258–261.
24. Takahashi A, Komiya E, Kakutani H, Yoshida T, Fujii M, et al. (2008) Domain mapping of a claudin-4 modulator, the C-terminal region of C-terminal fragment of *Clostridium perfringens* enterotoxin, by site-directed mutagenesis. Biochem Pharmacol 75: 1639–1648.
25. Meunier V, Bourrie M, Berger Y, Fabre G (1995) The human intestinal epithelial cell line Caco-2; pharmacological and pharmacokinetic applications. Cell Biol Toxicol 11: 187–194.
26. Hanna PC, Mietzner TA, Schoolnik GK, McClane BA (1991) Localization of the receptor-binding region of *Clostridium perfringens* enterotoxin utilizing cloned toxin fragments and synthetic peptides. J Biol Chem 266: 11037–11043.
27. Offner S, Hekele A, Teichmann U, Weinberger S, Gross S, et al. (2005) Epithelial tight junction proteins as potential antibody targets for pancarcinoma therapy. Cancer Immunol Immunother 54: 431–445.
28. Ling J, Liao H, Clark R, Wong MS, Lo DD (2008) Structural constraints for the binding of short peptides to claudin-4 revealed by surface plasmon resonance. J Biol Chem 283: 30585–30595.
29. Suzuki M, Kato-Nakano M, Kawamoto S, Furuya A, Abe Y, et al. (2009) Therapeutic antitumor efficacy of monoclonal antibody against Claudin-4 for pancreatic and ovarian cancers. Cancer Sci 100: 1623–1630.
30. Romani C, Comper F, Bandiera E, Ravaggi A, Bignotti E, et al. (2009) Development and characterization of a human single-chain antibody fragment against claudin-3: a novel therapeutic target in ovarian and uterine carcinomas. Am J Obstet Gynecol 201: 70 e71–79.
31. Furuse M, Furuse K, Sasaki H, Tsukita S (2001) Conversion of zonulae occludentes from tight to leaky strand type by introducing claudin-2 into Madin-Darby canine kidney I cells. J Cell Biol 153: 263–272.
32. Furuse M, Sasaki H, Tsukita S (1999) Manner of interaction of heterogeneous claudin species within and between tight junction strands. J Cell Biol 147: 891–903.
33. Umeda K, Ikenouchi J, Katahira-Tayama S, Furuse K, Sasaki H, et al. (2006) ZO-1 and ZO-2 independently determine where claudins are polymerized in tight-junction strand formation. Cell 126: 741–754.
34. Masuda K, Itoh H, Sakihama T, Akiyama C, Takahashi K, et al. (2003) A combinatorial G protein-coupled receptor reconstitution system on budded baculovirus. J Biol Chem 278: 24552–24562.
35. Hayashi I, Urano Y, Fukuda R, Isoo N, Kodama T, et al. (2004) Selective reconstitution and recovery of functional gamma-secretase complex on budded baculovirus particles. J Biol Chem 279: 38040–38046.
36. Saeki R, Kondoh M, Kakutani H, Tsunoda S, Mochizuki Y, et al. (2009) A novel tumor-targeted therapy using a claudin-4-targeting molecule. Mol Pharmacol 76: 918–926.

Claudin as a Target for Drug Development

A. Takahashi, M. Kondoh*, H. Suzuki and K. Yagi*

Graduate School of Pharmaceutical Sciences, Osaka University, Suita, Osaka 565-0871, Japan

Abstract: Tight junctions (TJs) play pivotal roles in the fence and barrier functions of epithelial and endothelial cell sheets. Since the 1980s, the modulation of the TJ barrier has been utilized as a method for drug absorption. Over the last decade, the structural and functional biochemical components of TJs, such as occludin and claudin, have been determined, providing new insights into TJ-based pharmaceutical therapy. For example, the modulation of the claudin barrier enhances the jejunal absorption of drugs, and claudin expression is deregulated in cancer cells. Claudin is a co-receptor for the hepatitis C virus. Moreover, claudin is modulated during inflammatory conditions. These findings indicate that claudins are promising drug targets. In this review, we discuss the seeds of claudin-based drug development, which may provide potential pharmaceutical breakthroughs in the future.

Keywords: Tight junction, claudin, cancer, inflammation, infection.

INTRODUCTION

Tight junctions (TJs) limit the movement of molecules through the intercellular space in epithelial and endothelial sheets, and they are located on the most apical part of cells [1, 2]. Electron microscopy has revealed that TJs appear as a series of continuous, anastomotic and intramembranous particle strands. Tsukita's group performed a series of biochemical analyses that clearly showed that the tetra-transmembrane proteins occludin and claudin are components of the TJ [3-5]. The claudin family contains more than 20 members. Interestingly, the expression profiles and the TJ-barrier function of the claudin family members are tissue-specific. For example, claudin-1 is involved in the epidermal barrier, and claudin-5 is involved in the blood-brain barrier [2, 6, 7]. It appears that claudin forms heteromeric and/or homomeric strands in TJs and that the combination and mixing ratios of different claudins determines the tissue-specific barrier properties of TJs [5, 8]. Epithelial cell sheets have bicellular TJs between adjacent cells and tricellular TJs at which three adjacent cells join together. Occludin and claudins are components of bicellular TJs. The occludin-related protein tricellulin has been recently identified to be a component of tricellular TJs [9]. Tricellulin is ubiquitously expressed in epithelial junctions of tissues and organs throughout the body. Down regulation of tricelluin mRNA by RNA interference resulted in disruption of epithelial barrier in an epithelial cell line [9]. However, human tricellulin mutations had no effect on epidermal, respiratory, renal or intestinal barrier [10]. Whether tricellulin can be a target for drug development is unclear.

Functions of TJs are classified as fence- and barrier- functions. Modulation of the TJ barrier has been a popular strategy used to promote drug absorption since the 1980s (See reviews [11, 12]). Sodium caprate is clinically used as an absorption enhancer of drug. Disturbance of either the TJ-fence function or the TJ-barrier function causes human diseases. Disturbance of the TJ-fence function followed by a loss of cellular polarity often occurs in tumorigenesis (See reviews [13-16]). TJs regulate the paracellular passage of ions, molecules, pathogens and inflammatory cells in epithelial and endothelial cell sheets [17-19]. The TJ-barrier becomes deregulated in various human diseases, including infections, inflammation and hereditary diseases (See reviews [20, 21]). Based on these findings, novel therapeutic strategies for TJ-related diseases have been proposed. In the present review, we discuss the seeds of claudin-based pharmaceutical therapies for human diseases relevant to TJs.

*Address correspondence to these authors at the Graduate School of Pharmaceutical Sciences, Osaka University, Suita, Osaka 565-0871, Japan; Tel: +81-6-6879-8196; Fax: +81-6-6879-8199; E-mail: masuo@phs.osaka-u.ac.jp

Tel: +81-6-6879-8195; Fax: +81-6-6879-8195; E-mail: yagi@phs.osaka-u.ac.jp

0929-8673/11 $58.00+.00

CANCER AND CLAUDIN

Malignant tumors are a major cause of death. Approximately 7.6 million people worldwide died from cancer in 2007, and 90% of tumors are derived from epithelial tissue [22]. Normal epithelial tissues develop cellular polarity, whereas the epithelial polarity is often deregulated during tumorigenesis [23]. TJs are localized between adjacent epithelial cells and separate the apical and basolateral membrane domains, which vary in protein and lipid content, resulting in the maintenance of the cell polarity. Claudins are deregulated in various cancers [13-16]. Claudin may regulate cancer metastasis by modulating activation of matrix metalloproteinases [11]. In this section, we discuss recent breakthroughs in claudin-targeted cancer therapy.

Claudin as a Diagnostic Marker

Claudin proteins are frequently overexpressed in ovarian cancers. In ovarian cancer cells with a high level of claudin-4, the critical claudin-4 promoter region exhibits a low level of DNA methylation and a high level of histone H3 acetylation [24]. Claudin-4 was detected in the 32 of 63 plasma samples of patients with ovarian cancers. Among 50 patients without ovarian cancer, only one had claudin-4–positive plasma. Thus, claudin-4 has a high specificity for the detection of ovarian cancers *via* a blood test, indicating that claudin-4 may be a diagnostic marker for ovarian cancer [25]. Because of the high specificity of claudin expression patterns in cancers, claudin might be a novel non-invasive diagnostic marker for cancer therapy.

Anti-Claudin Antibody

One of the most popular strategies for claudin-targeted cancer therapy is the preparation of antibody against the extracellular region of claudin. However, attempts to prepare anti-claudin antibodies have had little success because claudin has low antigenicity and is highly conserved in various species. A strain of autoimmune mice, BXSB, was immunized with a human pancreatic cancer cell line, resulting in the successful preparation of anti-claudin-4 monoclonal antibody that recognizes the extracellular region of claudin-4 [26, 27]. Moreover, the antibody mediated antibody-dependent cell cytotoxicity (ADCC) and *in vivo* anti-tumor activity. ScFv against the extracellular region of claudin-3 was isolated by using the ETH-2 Gold phage display library, which is a synthetic human recombinant antibody library that contains $>10^9$ possible antibody combinations in an scFv format [28, 29]. Immunization with DNA encoding the first extracellular loop of claudin-18 made success on preparation of anti-claudin-18 monoclonal antibody [30]. These successes in the preparation of anti-claudin antibody are likely to lead to a breakthrough in the development of claudin-targeted cancer therapy.

Clostridium Perfringens Enterotoxin

Another approach to targeting claudin in cancer therapy is the use of *Clostridium perfringens* enterotoxin (CPE) . CPE is a single-chain polypeptide of 35 kDa that causes food poisoning in humans. The functional domains of CPE consist of the N-terminal cytotoxic region and the C-terminal receptor-binding region [31]. Claudin-3 and -4 serve as the receptors for CPE. CPE binds to the second extracellular loop of claudin-3 and -4 [32] (Fig. **1**). We previously prepared a claudin-targeting molecule (C-CPE-PSIF) by fusion of the C-terminal fragment of CPE (C-CPE) with the protein synthesis inhibitory factor (PSIF) derived from *Pseudomonas aeruginosa* exotoxin. C-CPE-PSIF, but not PSIF, is cytotoxic to claudin-4 expressing cells. TJ-undeveloped cells are more sensitive to C-CPE-PSIF than TJ-developed cells. Polarized epithelial cells are sensitive to the basolaterally applied C-CPE-PSIF, but they are less sensitive to the apically applied C-CPE-PSIF. A claudin-targeting molecule may recognize the cellular polarity. Intratumoral injection of C-CPE-PSIF reduced tumor growth. These findings indicate that C-CPE may be a novel molecule for drug delivery and cancer therapy [33]. The receptor-binding region of C-CPE fused to TNF was cytotoxic in human ovarian cancer cells [34]. Thus, CPE fragments might be a tool for claudin-targeting therapy. Treatment of mice with claudin-3 siRNA suppressed ovarian tumor growth and metastasis [35]. Claudin gene silencing with siRNA is also potent anti-tumor agents.

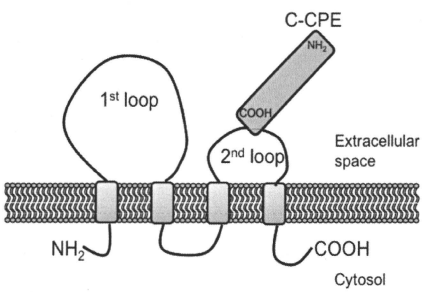

Fig. (1). Schematic illustration of interaction of C-CPE and claudin. Claudin is a tetra-transmembrane protein. C-CPE interacted with the 2nd loop region of claudin *via* its C-terminal domain [32, 76].

INFECTION AND CLAUDINS

Twenty million people die from infectious diseases each year. Most pathogens enter the body through nasal, pulmonary, intestinal and genital mucosa, and the mucosal epithelial cell sheets play a pivotal role as the first line of defense against the pathogens. Invading pathogens are distributed throughout the organ *via* endothelial cells of the blood vessels. TJs seal intercellular spaces between adjacent cells, preventing entry of the pathogens into the body and into the organ across the paracellular spaces. Disruption of mucosal TJ seals allows pathogens to enter into the body and the organ. In this section, we review the recent findings on the relationship between infections and claudins.

West Nile Virus (WNV) and Claudin

WNV, a neurotropic flavivirus, is a human pathogen that targets neurons and causes potentially lethal encephalitis in 1% to 2% of WNV-infected febrile patients [36]. No therapeutic agents or vaccines have been approved for use against WNV infection. Langerhans cells in the skin become infected with WNV by the bite of a carrier mosquito. WNV replicates in the regional tissues and lymph nodes, which results in the dissemination of the virus into the bloodstream. The following second replication proceeds at several sites in the host, including epithelial cells in the skin, kidney, intestine and testis, and then WNV may ultimately invade the brain [37]. The infection of the nervous system is characteristic of the most severe cases of WNV disease, and it often results in death or long-term neurologic sequelae [38]. Understanding the mechanism of the second infection and the viral entry into the brain is critical for the development of therapies against WNV. In WNV-infected epithelial cells, claudin-1, -2, -3 and -4 are degraded, followed by a disruption in the TJ barrier without cell death. The capsid of the WNV was responsible for the modulation of the TJ barrier [39]. These findings suggest that an inducer of claudin may be a promising candidate for pharmaceutical agents to inhibit the dissemination of WNV. Whether or not the WNV modulates the blood-brain barrier *via* the modulation of claudin-5 is an unsettled question.

Human Immunodeficiency Virus (HIV) and Claudin

HIV encephalitis (HIVE), including behavioral, motor, and cognitive impairments, is a common condition in the late stage of HIV-associated dementia [40]. Invasion of HIV into the brain and the transmigration of HIV-infected lymphocytes into the brain are the major causes of HIVE [41]. The blood-brain barrier (BBB), which is responsible for the regulation of solutes and cells between the peripheral circulation and the central nervous system, is comprised of the brain microvascular endothelial cells. Adjacent brain microvascular endothelial cells are connected by TJs that limit paracellular flux and restrict permeability [42]. The BBB frequently breaks down in patients with HIVE [41]. Claudin-5 plays a pivotal role in the BBB [7]. Treatment of human brain microvascular endothelial cells with HIV Gp120 envelope glycoprotein decreased the claudin-5 levels, followed by a disruption of the TJ barrier [43]. Claudin-5 levels were lower in brain microvessels from HIV patients with HIVE compared with brain microvessels from HIV patients without HIVE [44]. The deregulation of the claudin-5 barrier by HIV may be responsible for the breakdown of the BBB in HIV patients. Cannabinoids, the active ingredients in marijuana, reduce pain and improve the quality of life in HIV patients [45]. HIV activates signal transducers and activators of transcription-1 (STAT-1) [46]. Cannabinoids and an inhibitor of STAT-1 prevented the down-regulation of claudin-5 in the HIV Gp120- and HIV-treated human brain microvascular endothelial cells, respectively [43, 44]. These findings indicate that an inducer of claudin-5 may be a pharmaceutical agent for HIVE.

Hepatitis C Virus (HCV) and Claudin

Approximately 170 million people worldwide are infected with HCV. More than 80% of acute infections become persistent, resulting in liver fibrosis, cirrhosis, and hepatocellular carcinoma [47]. HCV infects human hepatocytes but not murine hepatocytes, and the detailed mechanism responsible for this difference has remained obscure. There is no pharmaceutical agent that prevents HCV infection. HCV attaches to tetraspanin CD81 and scavenger receptor class B type I (SR-BI) on host cells through its envelop glycoprotein [48, 49]. However, when CD81 and SR-BI were expressed in non-primate cell lines, the cells were still resistant to HCV entry [50, 51]. Recent studies to identify the additional factors that are needed to render non-human cells susceptible to HCV entry revealed that claudin-1 and occludin are co-receptors for HCV entry [51, 52]. HCV envelop proteins interact with the first extracellular loop region of claudin-1 and the second extracellular loop region of occludin [51, 52]. Binders to CD81, SR-BI, claudin-1 or/and occludin are expected to inhibit HCV entry. The HCV genome is frequently mutated; thus, pharmaceutical agents that recognize host molecules, such as the receptors, may be promising candidates for the prevention of HCV infection.

INFLAMMATORY BOWEL DISEASE (IBD) AND CLAUDIN

Inflammatory bowel disease (IBD), including ulcerative colitis and Crohn's disease, is characterized by an activated mucosal immune system that leads to impaired epithelial barrier function and tissue destruction with relapsing diarrhea [53, 54]. Ulcerative colitis is characterized by chronic inflammation and ulcers in the colon, while Crohn's disease causes ulcers and swelling of the mucosa on all areas of the digestive tract from the mouth to the anus. A common feature of IBD is enhanced permeability of the intestinal epithelium and disruption of the epithelial barrier. In this section, we summarize the recent findings on the relationship between IBD and claudins.

Changes of Claudins in IBD

The epithelial barrier function is impaired in ulcerative colitis, and ulcerative colitis is associated with decreased numbers of TJ strands in the epithelial barrier [55]. Biochemical analysis of TJ components in rectal biopsy specimens from patients with active ulcerative colitis revealed that the protein and mRNA levels of claudin-4 and -7 were decreased, whereas the protein and mRNA levels of claudin-2 were increased, as compared with control patients [56]. Overexpression of claudin-2 led to a decrease in the TJ barrier in an epithelial cell line, whereas claudin-4 or -7 transfection elevated the epithelial barrier function [57, 58]. Thus, the down-regulation of claudin-4/7 and the up-regulation of claudin-2 can lead to altered TJ structure, resulting in impaired epithelial function in active ulcerative colitis. However, claudin-deficient mice or claudin-overexpressing mice did not reproduce the pathology of IBD. Whether change in claudins is cause of IBD or result from IBD remains to be proved.

Although the precise etiology of IBD remains unknown, it is well accepted that IBD results from a deregulated mucosal immune response to environmental factors in genetically susceptible hosts. In IBD patients, the primary defect may be due to an abnormal intestinal epithelial barrier function [59]. The SAMP1/YitFc (SAMP) mouse strain is a spontaneous model of IBD that closely resembles Crohn's disease due to its histological features and localization to the terminal ileum [60]. The deregulated epithelial barrier function in SAMP mice is accompanied by an increase in claudin-2 and a decrease in occludin [61, 62].

FoxO4 is a member of the forkhead box transcription factor O (FoxO) subfamily, which has unique cell type–specific functions that regulate target genes and are involved in the regulation of immune responses [63, 64]. FoxO4-null mice were more susceptible to trinitrobenzene sulfonic acid–induced colitis [65]. FoxO4 deficiency increased the intestinal epithelial permeability and down-regulated the TJ proteins ZO-1 and claudin-1. Immunohistochemical analysis revealed that epithelial expression of FoxO4 was significantly down-regulated in patients with active ulcerative colitis as compared to patients with inactive ulcerative colitis [66]. Thus, FoxO4 might be a target for ulcerative colitis therapy.

A Potent Pharmaceutical Agent for IBD

Pro-inflammatory cytokines, such as tumor necrosis factor-α (TNF-α) and interferon-γ, are key mediators for the disruption of the epithelial barrier associated with Crohn's disease [55, 66, 67]. Expression of claudin-2 was increased by TNF-α in epithelial cells [68]. Experimental colitis model mice showed the down-regulation of occludin and up-regulation of claudin-2. Deletion of TNF-α receptor attenuated these changes of occludin and claudin-2 in the experimental colitis model. Importantly, anti-TNF treatment infliximab, which is currently used in Crohn's disease and ulcerative colitis, suppressed the reduction of occludin and elevation of claudin-2 in the experimental colitis model [69].

n-3 polyunsaturated fatty acids (PUFAs), which are abundant in fish oil and include eicosapentaenoic acid and docosahexaenoic acid, have beneficial effects on IBD [70-72]. In an experimental IBD model induced by treatment with trinitrobenzene sulfonic acid, the distribution of TJ proteins, including occludin and claudin-1, was affected; however, the administration of n-3 PUFAs prevented this redistribution of TJ proteins [73].

Probiotics are living bacteria that, when ingested in sufficient quantity, improve the health of the host beyond their inherent basic nutrition [74]. Probiotics have anti-inflammatory effects in IBD. VSL#3, a mixture of 8 probiotic bacterial strains, provided protection against intestinal inflammation in an experimental colitis model. Probiotics also attenuated the enhancement of epithelial permeability and the reduction of TJ components, including occludin, claudin-1 and -4 in the experimental model [75]. Therefore, compounds that enhance the TJ barrier function are candidates for IBD therapy.

CONCLUSIONS

Epithelium and endothelium are located between the outer and inner components of the body or tissues. Most malignant tumors are derived from epithelium. Moreover, epithelium and endothelium are also barriers that prevent invading pathogens and inflammatory cells from entering into the body and tissues. Therefore, the epithelium and endothelium are excellent targets for drug delivery systems, anti-tumor agents, anti-infection agents and anti-inflammatory agents.

Recent studies have revealed the involvement of claudin in some human diseases relevant to TJs (Table **1**). Claudin is often overexpressed in human cancers [13-16]. Therefore, a cancer therapy approach that uses claudin ligands is sought. Suzuki *et al.* used autoimmune mice to successfully prepare an anti-claudin-3 monoclonal antibody that mediated ADCC [26]. We anticipate that a novel claudin-targeted cancer therapy will be forthcoming. TJ components are also associated with infections. Claudin-1 and occludin are co-receptors for HCV [51, 52]. The claudin-5 level was reduced in brain microvessels of patients with HIVE [44], and cannabinoids, a clinically used agent for HIV patients, prevented the down-regulation of claudin-5 [43]. These findings indicate that a

Table 1. Perspective on Claudin-Targeted Therapies

Applications	Claudins	References
A diagnostic marker for ovarian cancers	Claudin-4	[25]
Inhibitor of WNV dissemination	Claudin-1~4	[39]
Inhibitor of HIV encephalitis	Claudin-5	[43-45]
Inhibitor of HCV infection	Claudin-1	[51]
Inhibitor of intestinal inflammation in IBD	Claudin-1~4	[69, 73, 75]

WNV, west nile virus; HIV, human immunodeficiency virus; HCV, hepatitis C virus; IBD, inflammatory bowel disease.

claudin/occludin binder and an inducer of claudin-5 may be an inhibitor of HCV infection and a therapeutic agent for HIVE patients. Disruption of the intestinal epithelial barrier is a common feature in patients with IBD. A chemical compound that strengthens the claudin barrier function will be a promising drug for IBD.

Biochemical and functional information regarding TJs has accumulated since the identification of occludin in 1993, and the deregulation of claudins has been observed in several human diseases [16, 20, 21]. The potential of TJ-based therapies is promising. We believe that TJ-targeted therapies might provide a breakthrough in pharmaceutical therapy in the future.

ACKNOWLEDGEMENTS

We also thank the members of our laboratory for their useful comments and discussion. Our work referred in this review was partly supported by MEXT KAKENHI (21689006), by a Health and Labor Sciences Research Grants from the Ministry of Health, Labor and Welfare of Japan, by Takeda Science Foundation, by a Suzuken Memorial Foundation and by a grant from Kansai Biomedical Cluster project in Saito, which is promoted by the Knowledge Cluster Initiative of the Ministry of Education, Culture, Sports, Science and Technology, Japan. A.T. is supported by Research Fellowships of the Japan Society for the Promotion of Science for Young Scientists.

ABBREVIATIONS

TJ	=	Tight junction
ADCC	=	antibody-dependent cell cytotoxicity
CPE	=	*Clostridium perfringens* enterotoxin
C-CPE	=	the C-terminal fragment of CPE
PSIF	=	protein synthesis inhibitory factor
WNV	=	West Nile virus
HIV	=	human immunodeficiency virus
HIVE	=	HIV encephalitis
BBB	=	blood-brain barrier
STAT-1	=	signal transducers and activators of transcription-1
HCV	=	hepatitis C virus
SR-BI	=	scavenger receptor class B type I
IBD	=	inflammatory bowel disease
FoxO	=	forkhead box transcription factor O
TNF	=	tumor necrosis factor
PUFAs	=	n-3 polyunsaturated fatty acids

REFERENCES

[1] Anderson, J. Molecular structure of tight junctions and their role in epithelial transport. *News Physiol. Sci.*, **2001**, *16*, 126-130.

[2] Tsukita, S.; Furuse, M.; Itoh, M. Multifunctional strands in tight junctions. *Nat. Rev. Mol. Cell Biol.*, **2001**, *2*, 285-293.

[3] Furuse, M.; Fujita, K.; Hiiragi, T.; Fujimoto, K.; Tsukita, S. Claudin-1 and -2: novel integral membrane proteins localizing at tight junctions with no sequence similarity to occludin. *J. Cell Biol.*, **1998**, *141*, 1539-1550.

[4] Furuse, M.; Hirase, T.; Itoh, M.; Nagafuchi, A.; Yonemura, S.; Tsukita, Sa.; Tsukita, Sh. Occludin: a novel integral membrane protein localizing at tight junctions. *J. Cell Biol.*, **1993**, *123*, 1777-1788.

[5] Furuse, M.; Tsukita, S. Claudins in occluding junctions of humans and flies. *Trends Cell Biol.*, **2006**, *16*, 181-188.

[6] Furuse, M.; Hata, M.; Furuse, K.; Yoshida, Y.; Haratake, A.; Sugitani, Y.; Noda, T.; Kubo, A.; Tsukita, S. Claudin-based tight junctions are crucial for the mammalian epidermal barrier: a lesson from claudin-1-deficient mice. *J. Cell Biol.*, **2002**, *156*, 1099-1111.

[7] Nitta, T.; Hata, M.; Gotoh, S.; Seo, Y.; Sasaki, H.; Hashimoto, N.; Furuse, M.; Tsukita, S. Size-selective loosening of the blood-brain barrier in claudin-5-deficient mice. *J. Cell Biol.*, **2003**, *161*, 653-660.

[8] Furuse, M.; Sasaki, H.; Tsukita, S. Manner of interaction of heterogeneous claudin species within and between tight junction strands. *J. Cell Biol.*, **1999**, *147*, 891-903.

[9] Ikenouchi, J.; Furuse, M.; Furuse, K.; Sasaki, H.; Tsukita, Sa.; Tsukida, Sh. Tricellulin constitutes a novel barrier at tricellular contacts of epithelial cells. *J. Cell Biol.*, **2005**, 171, 939-945.

[10] Riazuddin, S.; Ahmed, Z.M.; Fanning, A.S.; Lagziel, A.; Kitajiri, S.; Ramzan, K.; Khan, S.N.; Chattaraj, P.; Friedman, P.L.; Anderson, J.M.; Belyantseva, I.A.; Forge, A.; Riazuddin, S.; Friedman, T.B. Tricellulin is a tight-junction protein necessary for hearing. *Am. J. Hum. Genet.*, **2006**, 79, 1040-1051.

[11] Kondoh, M.; Yoshida, T.; Kakutani, H.; Yagi, K. Targeting tight junction proteins-significance for drug development. *Drug Discov. Today,* **2008**, *13*, 180-186.

[12] Matsuhisa, K.; Kondoh, M.; Takahashi, A.; Yagi, K. Tight junction modulator and drug delivery. *Expert Opin. Drug Deliv.*, **2009**, *6*, 509-515.

[13] Kominsky, S.L. Claudins: emerging targets for cancer therapy. *Expert Rev. Mol. Med.*, **2006**, *8*, 1-11.

[14] Morin, P.J. Claudin proteins in human cancer: promising new targets for diagnosis and therapy. *Cancer Res.*, **2005**, *65*, 9603-9606.

[15] Swisshelm, K.; Macek, R.; Kubbies, M. Role of claudins in tumorigenesis. *Adv. Drug Deliv. Rev.*, **2005**, *57*, 919-928.

[16] Tsukita, Sa.; Yamazaki, Y.; Katsuno, T.; Tamura, A.; Tsukita, Sh. Tight junction-based epithelial microenvironment and cell proliferation. *Oncogene,* **2008**, *27*, 6930-6938.

[17] Schulzke, D.; Ploeger, S.; Amasheh, M.; Fromm, A.; Zeissig, S.; Troeger, H.; Richter, J.; Bojarski, C.; Schumann, M.; Fromm, M. Epithelial tight junctions in intestinal inflammation. *Ann. N.Y. Acad. Sci.*, **2009**, 1165, 294-300.

[18] Van Itallie, C.M.; Betts, L.; Smedley, J.G.3rd; McClane, B.A.; Anderson, J.M. Structure of the claudin-binding domain of *Clostridium perfringens* enterotoxin. *J. Biol. Chem.*, **2008**, 283, 268-274.

[19] Argaw, A.T.; Gurfein, B.T.; Zhang, Y.; Zameer, A.; John, G.R. VEGF-mediated disruption of endothelial CLN-5 promotes blood-brain barrier breakdown. *Proc. Natl. Acad. Sci. USA*, **2009**, 106, 1977-1982.

[20] Furuse, M. Knockout animals and natural mutations as experimental and diagnostic tool for studying tight junction functions *in vivo*. *Biochim. Biophys. Acta.*, **2009**, *1788*, 813-819.

[21] Sawada, N.; Murata, M.; Kikuchi, K.; Osanai, M.; Tobioka, H.; Kojima, T.; Chiba, H. Tight junctions and human diseases. *Med. Electron. Microsc.*, **2003**, *36*, 147-156.

[22] Jemal, A.; Siegel, R.; Ward, E.; Hao, Y.; Xu, J.; Murray, T.; Thun, M.J. Cancer statistics, 2008. *CA Cancer J. Clin.*, **2008**, *58*, 71-96.

[23] Wodarz, A.; Nathke, I. Cell polarity in development and cancer. *Nat. Cell Biol.*, **2007**, *9*, 1016-1024.

[24] Honda, H.; Pazin, M.J.; Ji, H.; Wernyj, R.P.; Morin, P.J. Crucial roles of Sp1 and epigenetic modifications in the regulation of the CLDN4 promoter in ovarian cancer cells. *J. Biol. Chem.*, **2006**, *281*, 21433-21444.

[25] Li, J.; Sherman-Baust, C.A.; Tsai-Turton, M.; Bristow, R.E.; Roden, R.B.; Morin, P.J. Claudin-containing exosomes in the peripheral circulation of women with ovarian cancer. *BMC Cancer,* **2009**, *9*, 244.

[26] Suzuki, M.; Kato-Nakano, M.; Kawamoto, S.; Furuya, A.; Abe, Y.; Misaka, H.; Kimoto, N.; Nakamura, K.; Ohta, S.; Ando, H. Therapeutic antitumor efficacy of monoclonal antibody against Claudin-4 for pancreatic and ovarian cancers. *Cancer Sci.*, **2009**, *100*, 1623-1630.

[27] Yin, B.W.; Wong, G.Y.; Lloyd, K.O.; Oettgen, H.F.; Welt, S. Increased yields of IgG2a- and IgG3-secreting hybridomas after fusion of B cells from mice with autoimmune diseases. *J. Immunol. Methods,* **1991**, *144*, 165-173.

[28] Pini, A.; Viti, F.; Santucci, A.; Carnemolla, B.; Zardi, L.; Neri, P.; Neri, D. Design and use of a phage display library. Human antibodies with subnanomolar affinity against a marker of angiogenesis eluted from a two-dimensional gel. *J. Biol. Chem.*, **1998**, *273*, 21769-21776.

[29] Romani, C.; Comper, F.; Bandiera, E.; Ravaggi, A.; Bignotti, E.; Tassi, R.A.; Pecorelli, S.; Santin, A.D. Development and characterization of a human single-chain antibody fragment against claudin-3: a novel therapeutic target in ovarian and uterine carcinomas. *Am. J. Obstet. Gynecol.*, **2009**, *201*, 70. e71-79.

[30] Sahin, U.; Koslowski, M.; Dhaene, K.; Usener, D.; Brandenburg, G.; Seitz, G.; Huber, C.; Tureci, O. Claudin-18 splice variant 2 is a pan-cancer target suitable for therapeutic antibody development. *Clin. Cancer Res.*, **2008**, *14*, 7624-7634.

[31] Hanna, P.C.; Wieckowski, E.U.; Mietzner, T.A.; McClane, B.A. Mapping of functional regions of *Clostridium perfringens* type A enterotoxin. *Infect. Immun.*, **1992**, *60*, 2110-2114.

[32] Fujita, K.; Katahira, J.; Horiguchi, Y.; Sonoda, N.; Furuse, M.; Tsukita, S. *Clostridium perfringens* enterotoxin binds to the second extracellular loop of claudin-3, a tight junction integral membrane protein. *FEBS Lett.*, **2000**, *476*, 258-261.

[33] Saeki, R.; Kondoh, M.; Kakutani, H.; Tsunoda, S.; Mochizuki, Y.; Hamakubo, T.; Tsutsumi, Y.; Horiguchi, Y.; Yagi, K. A novel tumor-targeted therapy using a claudin-4-targeting molecule. *Mol. Pharmacol.*, **2009**, *76*, 918-926.

[34] Yuan, X.; Lin, X.; Manorek, G.; Kanatani, I.; Cheung, L.H.; Rosenblum, M.G.; Howell, S.B. Recombinant CPE fused to tumor necrosis factor targets human ovarian cancer cells expressing the claudin-3 and claudin-4 receptors. *Mol. Cancer Ther.*, **2009**, *8*, 1906-1915.

[35] Huang, Y.H.; Bao, Y.; Peng, W.; Goldberg, M.; Love, K.; Bumcrot, D.A.; Cole, G.; Langer, R.; Anderson, D.G.; Swicki, J.A. Claudin-3 gene silencing with siRNA suppresses ovarian tumor growth and metastasis. *Proc. Natl. Acad. Sci. USA*, **2009**, 106, 3426-3430.

[36] Hayes, E.B.; Gubler, D.J. West Nile virus: epidemiology and clinical features of an emerging epidemic in the United States. *Annu. Rev. Med.*, **2006**, *57*, 181-194.

[37] Samuel, M.A.; Diamond, M.S. Pathogenesis of West Nile Virus infection: a balance between virulence, innate and adaptive immunity, and viral evasion. *J. Virol.*, **2006**, *80*, 9349-9360.

[38] Klee, A.L.; Maidin, B.; Edwin, B.; Poshni, I.; Mostashari, F.; Fine, A.; Layton, M.; Nash, D. Long-term prognosis for clinical West Nile virus infection. *Emerg. Infect. Dis.*, **2004**, *10*, 1405-1411.

[39] Medigeshi, G.R.; Hirsch, A.J.; Brien, J.D.; Uhrlaub, J.L.; Mason, P.W.; Wiley, C.; Nikolich-Zugich, J.; Nelson, J.A. West nile virus capsid degradation of claudin proteins disrupts epithelial barrier function. *J. Virol.*, **2009**, *83*, 6125-6134.

[40] McArthur, J.C. HIV dementia: an evolving disease. *J. Neuroimmunol.*, **2004**, *157*, 3-10.

[41] Banks, W.A.; Ercal, N.; Price, T.O. The blood-brain barrier in neuroAIDS. *Curr. HIV Res.*, **2006**, *4*, 259-266.

[42] Hawkins, B.T.; Davis, T.P. The blood-brain barrier/neurovascular unit in health and disease. *Pharmacol. Rev.*, **2005**, *57*, 173-185.

[43] Lu, T.S.; Avraham, H.K.; Seng, S.; Tachado, S.D.; Koziel, H.; Makriyannis, A.; Avraham, S. Cannabinoids inhibit HIV-1 Gp120-mediated insults in brain microvascular endothelial cells. *J. Immunol.*, **2008**, *181*, 6406-6416.

[44] Chaudhuri, A.; Yang, B.; Gendelman, H.E.; Persidsky, Y.; Kanmogne, G.D. STAT1 signaling modulates HIV-1-induced inflammatory responses and leukocyte transmigration across the blood-brain barrier. *Blood*, **2008**, *111*, 2062-2072.

[45] Pacher, P.; Batkai, S.; Kunos, G. The endocannabinoid system as an emerging target of pharmacotherapy. *Pharmacol. Rev.*, **2006**, *58*, 389-462.

[46] Bovolenta, C.; Camorali, L.; Lorini, A.L.; Ghezzi, S.; Vicenzi, E.; Lazzarin, A.; Poli, G. Constitutive activation of STATs upon *in vivo* human immunodeficiency virus infection. *Blood*, **1999**, *94*, 4202-4209.

[47] Poynard, T.; Yuen, M.F.; Ratziu, V.; Lai, C.L. Viral hepatitis C. *Lancet*, **2003**, *362*, 2095-2100.

[48] Pileri, P.; Uematsu, Y.; Campagnoli, S.; Galli, G.; Falugi, F.; Petracca, R.; Weiner, A.J.; Houghton, M.; Rosa, D.; Grandi, G.; Abrignani, S. Binding of hepatitis C virus to CD81. *Science*, **1998**, *282*, 938-941.

[49] Scarselli, E.; Ansuini, H.; Cerino, R.; Roccasecca, R.M.; Acali, S.; Filocamo, G.; Traboni, C.; Nicosia, A.; Cortese, R.; Vitelli, A. The human scavenger receptor class B type I is a novel candidate receptor for the hepatitis C virus. *Embo. J.*, **2002**, *21*, 5017-5025.

[50] Bartosch, B.; Dubuisson, J.; Cosset, F.L. Infectious hepatitis C virus pseudoparticles containing functional E1-E2 envelope protein complexes. *J. Exp. Med.*, **2003**, *197*, 633-642.

[51] Evans, M.J.; von Hahn, T.; Tscherne, D.M.; Syder, A.J.; Panis, M.; Wolk, B.; Hatziioannou, T.; McKeating, J.A.; Bieniasz, P.D.; Rice, C.M. Claudin-1 is a hepatitis C virus co-receptor required for a late step in entry. *Nature*, **2007**, *446*, 801-805.

[52] Ploss, A.; Evans, M.J.; Gaysinskaya, V.A.; Panis, M.; You, H.; de Jong, Y.P.; Rice, C.M. Human occludin is a hepatitis C virus entry factor required for infection of mouse cells. *Nature*, **2009**, *457*, 882-886.

[53] Gitter, A.H.; Wullstein, F.; Fromm, M.; Schulzke, J.D. Epithelial barrier defects in ulcerative colitis: characterization and quantification by electrophysiological imaging. *Gastroenterology*, **2001**, *121*, 1320-1328.

[54] Marin, M.L.; Greenstein, A.J.; Geller, S.A.; Gordon, R.E.; Aufses, A.H., Jr. A freeze fracture study of Crohn's disease of the terminal ileum: changes in epithelial tight junction organization. *Am. J. Gastroenterol.*, **1983**, *78*, 537-547.

[55] Schmitz, H.; Barmeyer, C.; Fromm, M.; Runkel, N.; Foss, H.D.; Bentzel, C.J.; Riecken, E.O.; Schulzke, J.D. Altered tight junction structure contributes to the impaired epithelial barrier function in ulcerative colitis. *Gastroenterology*, **1999**, *116*, 301-309.

[56] Oshima, T.; Miwa, H.; Joh, T. Changes in the expression of claudins in active ulcerative colitis. *J. Gastroenterol. Hepatol.*, **2008**, *23 Suppl 2*, S146-150.

[57] Alexandre, M.D.; Lu, Q.; Chen, Y.H. Overexpression of claudin-7 decreases the paracellular Cl- conductance and increases the paracellular Na+ conductance in LLC-PK1 cells. *J. Cell Sci.*, **2005**, *118*, 2683-2693.

[58] Van Itallie, C.; Rahner, C.; Anderson, J.M. Regulated expression of claudin-4 decreases paracellular conductance through a selective decrease in sodium permeability. *J. Clin. Invest.*, **2001**, *107*, 1319-1327.

[59] Shorter, R.G.; Huizenga, K.A.; Spencer, R.J.; Guy, S.K. Inflammatory bowel disease. The role of lymphotoxin in the cytotoxicity of lymphocytes for colonic epithelial cells. *Am. J. Dig. Dis.*, **1972**, *17*, 689-696.

[60] Kosiewicz, M.M.; Nast, C.C.; Krishnan, A.; Rivera-Nieves, J.; Moskaluk, C.A.; Matsumoto, S.; Kozaiwa, K.; Cominelli, F. Th1-type responses mediate spontaneous ileitis in a novel murine model of Crohn's disease. *J. Clin. Invest.*, **2001**, *107*, 695-702.

[61] Reuter, B.K.; Pizarro, T.T. Mechanisms of tight junction dysregulation in the SAMP1/YitFc model of Crohn's disease-like ileitis. *Ann. N.Y. Acad. Sci.*, **2009**, *1165*, 301-307.

[62] Vidrich, A.; Buzan, J.M.; Barnes, S.; Reuter, B.K.; Skaar, K.; Ilo, C.; Cominelli, F.; Pizarro, T.; Cohn, S.M. Altered epithelial cell lineage allocation and global expansion of the crypt epithelial stem cell population are associated with ileitis in SAMP1/YitFc mice. *Am. J. Pathol.*, **2005**, *166*, 1055-1067.

[63] Paik, J.H.; Kollipara, R.; Chu, G.; Ji, H.; Xiao, Y.; Ding, Z.; Miao, L.; Tothova, Z.; Horner, J.W.; Carrasco, D.R.; Jiang, S.; Gilliland, D.G.; Chin, L.; Wong, W.H.; Castrillon, D.H.; DePinho, R.A. FoxOs are lineage-restricted redundant tumor suppressors and regulate endothelial cell homeostasis. *Cell*, **2007**, *128*, 309-323.

[64] Tothova, Z.; Kollipara, R.; Huntly, B.J.; Lee, B.H.; Castrillon, D.H.; Cullen, D.E.; McDowell, E.P.; Lazo-Kallanian, S.; Williams, I.R.; Sears, C.; Armstrong, S.A.; Passegue, E.; DePinho, R.A.; Gilliland, D.G. FoxOs are critical mediators of hematopoietic stem cell resistance to physiologic oxidative stress. *Cell*, **2007**, *128*, 325-339.

[65] Zhou, W.; Cao, Q.; Peng, Y.; Zhang, Q.J.; Castrillon, D.H.; DePinho, R.A.; Liu, Z.P. FoxO4 inhibits NF-kappaB and protects mice against colonic injury and inflammation. *Gastroenterology*, **2009**, *137*, 1403-1414.

[66] Gitter, A.H.; Bendfeldt, K.; Schulzke, J.D.; Fromm, M. Leaks in the epithelial barrier caused by spontaneous and TNF-alpha-induced single-cell apoptosis. *Faseb. J.*, **2000**, *14*, 1749-1753.

[67] Mankertz, J.; Tavalali, S.; Schmitz, H.; Mankertz, A.; Riecken, E.O.; Fromm, M.; Schulzke, J.D. Expression from the human occludin promoter is affected by tumor necrosis factor alpha and interferon gamma. *J. Cell. Sci.*, **2000**, *113*, 2085-2090.

[68] Mankertz, J.; Amasheh, M.; Krug, S.M.; Fromm, A.; Amasheh, S.; Hillenbrand, B.; Tavalali, S.; Fromm, M.; Schulzke, J.D. TNFalpha up-regulates claudin-2 expression in epithelial HT-29/B6 cells *via* phosphatidylinositol-3-kinase signaling. *Cell Tissue Res.*, **2009**, *336*, 67-77.

[69] Fries, W.; Muja, C.; Crisafulli, C.; Cuzzocrea, S.; Mazzon, E. Dynamics of enterocyte tight junctions: effect of experimental colitis and two different anti-TNF strategies. *Am. J. Physiol.*, **2008**, *294*, G938-947.

[70] Aslan, A.; Triadafilopoulos, G. Fish oil fatty acid supplementation in active ulcerative colitis: a double-blind, placebo-controlled, crossover study. *Am. J. Gastroenterol.*, **1992**, *87*, 432-437.

[71] Hawthorne, A.B.; Daneshmend, T.K.; Hawkey, C.J.; Belluzzi, A.; Everitt, S.J.; Holmes, G.K.; Malkinson, C.; Shaheen, M.Z.; Willars, J.E. Treatment of ulcerative colitis with fish oil supplementation: a prospective 12 month randomised controlled trial. *Gut*, **1992**, *33*, 922-928.

[72] Kitsukawa, Y.; Saito, H.; Suzuki, Y.; Kasanuki, J.; Tamura, Y.; Yoshida, S. Effect of ingestion of eicosapentaenoic acid ethyl ester on carrageenan-induced colitis in guinea pigs. *Gastroenterology*, **1992**, *102*, 1859-1866.

[73] Li, Q.; Zhang, Q.; Zhang, M.; Wang, C.; Zhu, Z.; Li, N.; Li, J. Effect of n-3 polyunsaturated fatty acids on membrane microdomain localization of tight junction proteins in experimental colitis. *Febs. J.*, **2008**, *275*, 411-420.

[74] Fuller, R. Probiotics in man and animals. *J. Appl. Bacteriol.*, **1989**, *66*, 365-378.

[75] Mennigen, R.; Nolte, K.; Rijcken, E.; Utech, M.; Loeffler, B.; Senninger, N.; Bruewer, M. Probiotic mixture VSL#3 protects the epithelial barrier by maintaining tight junction protein expression and preventing apoptosis in a murine model of colitis. *Am. J. Physiol.*, **2009**, *296*, G1140-1149.

[76] Takahashi, A.; Kondoh, M.; Masuyama, A.; Fujii, M.; Mizuguchi, H.; Horiguchi, Y.; Watanabe, Y. Role of C-terminal regions of the C-terminal fragment of *Clostridium perfringens* enterotoxin in its interaction with claudin-4. *J. Control. Release*, **2005**, *108*, 56-62.

Received: December 26, 2010 **Revised: March 28, 2011** **Accepted: March 29, 2011**

Journal of Controlled Release 149 (2011) 36–41

Contents lists available at ScienceDirect

Journal of Controlled Release

journal homepage: www.elsevier.com/locate/jconrel

Review

Progress in the development of ultrasound-mediated gene delivery systems utilizing nano- and microbubbles

Ryo Suzuki, Yusuke Oda, Naoki Utoguchi, Kazuo Maruyama *

Department of Biopharmaceutics, School of Pharmaceutical Sciences, Teikyo University, 1091-1 Suwarashi, Midori-ku, Sagamihara, Kanagawa 252-5195, Japan

ARTICLE INFO

Article history:
Received 28 December 2009
Accepted 6 May 2010
Available online 12 May 2010

Keywords:
Ultrasound
Microbubbles
Sonoporation
Gene delivery
Cavitation

ABSTRACT

Recently, ultrasound-mediated gene delivery with nano- and microbubbles was developed as a novel non-viral vector system. In this gene delivery system, microstreams and microjets, which are induced by disruption of nano/microbubbles exposed to ultrasound, are used as the driving force to transfer genes into cells by opening transient pores in the cell membrane. This system can directly deliver plasmid DNA and siRNA into cytosol without endocytosis pathway. Therefore, these genes are able to escape from degradation in lysosome and result in enhancing the efficiency of gene expression. In addition, it is expected that ultrasound-mediated gene delivery using nano/microbubbles would be a system to establish non-invasive and tissue specific gene expression because ultrasound can transdermally expose to target tissues and organs. This review focuses on the current ultrasound-mediated gene delivery system using nano/microbubbles. We discuss about the feasibility of this gene delivery system as novel non-viral vector system.

Contents

1. Introduction

Gene therapy has a potential in the treatment of cancer and diseases that are due to genomic causes. Viral vectors are efficient carriers of genes for transduction, but some problems have become evident [1–3]. Delivery vectors that are highly potent in terms of gene transduction efficiency should also be safe and easy to apply. Non-viral vectors have recently received focus as gene carriers, but their transduction efficiency is very low. Efforts have recently been directed towards improving this aspect [4–6]. Towards this end, ultrasound has been investigated for improving the efficiency of transgene delivery, and holds promise as a non-invasive gene delivery system.

Ultrasound shows potential for improving the efficiency of gene delivery into tissues and cells, a technique known as sonophoresis/sonoporation [7]. It is believed that ultrasound perturbs cell membranes and causes transient pores to open in the membrane, thus facilitating gene entry into the cell [8]. In addition, it has been reported that microbubbles utilized as ultrasound contrast agents play an important role in enhancing the efficiency of gene delivery, without causing cell damage [9]. In general, cell damage is dependent on ultrasound intensity, concentration of microbubbles and cell type. Especially, ultrasound intensity and exposure time are key factors. Therefore, it is important to optimize the condition of ultrasound exposure in ultrasound-mediated gene delivery [10–13]. Some researchers studied about the cell damage by the disruption of microbubbles with ultrasound exposure [14–19]. These reports are useful as informative references for ultrasound-mediated gene delivery utilizing microbubbles.

* Corresponding author. Tel.: +81 42 685 3722; fax: +81 42 685 3432.
E-mail address: maruyama@pharm.teikyo-u.ac.jp (K. Maruyama).

0168-3659/$ – see front matter
doi:10.1016/j.jconrel.2010.05.009

Microbubbles which are destroyed by ultrasound exposure generate microstreams or microjets, resulting in shear stress to cells and the generation of transient holes in cell membranes [20]. Since this approach can be used to deliver extracellular molecules such as genes into cells, microbubbles could facilitate ultrasound-mediated gene delivery. In addition, submicron sized bubbles (nanobubbles), which are smaller than conventional microbubbles, were recently reported [21,22], and we have also developed novel liposomal nanobubbles (Bubble liposomes) [11,23–32]. These nanobubbles can also be utilized as enhancing tool of gene delivery efficiency in ultrasound-mediated gene delivery. In this review, we introduced about ultrasound-mediated delivery systems combined with nano/microbubbles and discussed the feasibility as non-viral vector system.

2. Microbubbles as ultrasound contrast agents

Ultrasonography is a widely used diagnostic medical imaging technique that is non-invasive, relatively low-cost, easy to use, provides real-time imaging, and importantly, avoids the use of hazardous ionizing radiation. Ultrasound wave pulses generated by an ultrasound transducer are partially reflected or scattered by the interfaces between different tissues. The transducer detects the ultrasound waves returned by scattering, and these signals are converted to ultrasound images. Since blood scatters ultrasound poorly, ultrasound contrast agents, which increase the scattering and reflection of ultrasound waves, are utilized for blood flow imaging, especially in cardiosonography. Gramiak and Shah in 1968 were the first to use contrast agents in echocardiography [33], and reported that the aortic delineation was improved by intracardiac injection of agitated saline containing air bubbles. However, these air microspheres disappeared within a few seconds following intravenous injection due to the high solubility of air in blood, and the impossibility of larger air bubbles to pass through pulmonary capillaries. For these reasons, it is difficult to use injected conventional air bubbles for opacifying the left cardiac chambers, unless they are injected by the intracoronary or aortic route.

To improve the stability and decrease the size of air bubbles, microbubbles with a thin shell such as albumin (Albunex) or galactose palmitic acid (Levovist) have been developed (Table 1). These bubbles are first-generation microbubbles, and are air-filled microspheres. Their mean diameter ranges from 1 to 8 μm, and they are capable of passing through pulmonary capillaries. However, these air-filled microbubbles disappear from the bloodstream within seconds after administration because of their low resistance to arterial pressure gradients, and the high solubility of air in blood [34]. Approaches for increasing the stability of microbubbles and decreasing the solubility of their gas in blood are clearly required, and lead to the development of microbubbles filled with a high molecular weight hydrophobic gas such as perfluorocarbons or sulfur hexafluoride. These microbubbles represent second-generation contrast agents, in which surfactants, sonicated albumin and phospholipids are used to form the bubble shell in order to improve microbubble stability in the bloodstream. The acoustic backscatter of these microbubbles is higher than that of blood and organs, due to differences in acoustic impedance between gases, and blood or organs. Therefore, microbubbles are useful contrast agents, especially in echocardiography. In addition, Sonazoid which was a phosphatidylserine-stabilized perfluorobutane microbubbles was developed as a useful contrast agent for hepatic tumors [35–37]. This is due to uniqueness of Sonazoid whose microbubbles are likely to be taken up by Kupffer cells (liver macrophages) in the healthy liver and enhances contrast of the liver parenchyma during the delayed phase, which usually occurs within 10 min after the injection. In contrast, tumor that lacks Kupffer cells was not enhanced resulting in clear negative contrast of the tumor [36]. Thus, Sonazoid is a new type of microbubble which is able to target Kupffer cells. However, Sonazoid has been commercially available microbubble for clinical use only in Japan since 2007. In the future, it is expected that tissue specific targeting bubbles such as Sonazoid are developed.

Table 1
Ultrasound contrast agents.

Name	Shell	Entrapping gas	Size (μm)
Albunex	Albumin	Air	4.3
Levovist	Galactose	Air	2–4
Optison	Albumin	Perfluoropropane	3–32
Definity	Lipids	Perfluoropropane	1.1–20
Imagent	Lipids	Perfluoropropane	5
Sonovue	Lipids	Sulphur hexafluoride	2.5
Sonazoid	Lipids	Perfluorobutane	2–3

3. Properties of microbubbles combined with ultrasound

The behavior of microbubbles depends on the amplitude of ultrasound used. At very low acoustic pressure (mechanical index (MI)<0.05–0.1), the microbubbles cause linear oscillation, and the reflected frequency is equal to the transmitted frequency (Fig. 1(a)). An increase in acoustic pressure (0.1<MI<0.3), referred to as low-power imaging, causes non-linear expansion and compression of the microbubbles (Fig. 1(b)). In fact, the bubble becomes somewhat more resistant to compression than to expansion. This phenomenon is known as stable or non-inertial cavitation, and results in the emission of non-linear harmonic signals at multiples of the transmitted frequency [38]. Harmonic imaging with microbubbles enhances the bubbles-to-tissue backscatter signal ratio, due to insignificant harmonic backscatter from tissue in this range of MI. Therefore, this technique can improve the signal-noise ratio and be useful in left ventricular pacification imaging [39]. In addition, stable or non-inertial cavitation can enhance transient cell membrane permeability (Fig. 2(a)) [40]. Machluf et al. reported that ultrasound exposure (0.16 MI, 1 MHz) in the presence of microbubbles deliver plasmid DNA into cells [41,42].

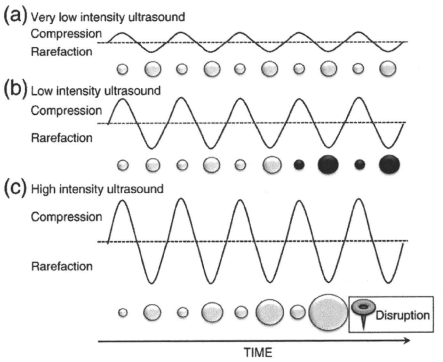

Fig. 1. Scheme showing microbubble behavior in acoustic fields (a) Very low intensity ultrasound induces linear oscillation of the microbubble. (b) Low intensity ultrasound induces oscillation of the microbubble with a gradual increase in microbubble diameter until it reaches a resonant diameter, at which point stable oscillation occurs (filled black circles). (c) High intensity ultrasound causes a rapid increase in the diameter of the microbubble for a few cycles, which induces bubble disruption.

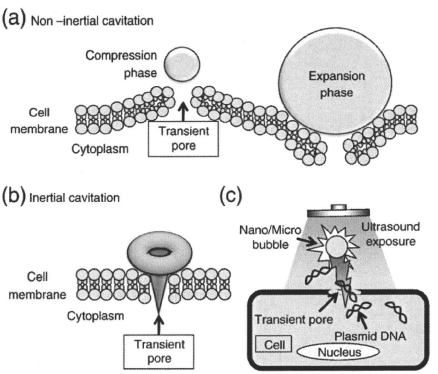

Fig. 2. Scheme showing the pore formation in the cell membrane by oscillating or disrupting microbubble (a) The pushing and pulling behavior (non-inertial cavitation) of the microbubble and (b) the collapse of microbubbles (inertial cavitation) cause rupture of the cell membrane creating pore allowing trans-membrane flux of fluid and macromolecules such as plasmid DNA and oligonucleotides (c).

Higher acoustic pressure (MI>0.3–0.6) causes forced expansion and compression of microbubbles and results in bubble disruption (collapse) (Fig. 1(c)). This inertial cavitation involved in bubble disruption is utilized as flash-replenishment in reperfusion study of diagnosis [43]. This inertial cavitation induces microstreams/microjets around the bubbles. The peak velocity of the microstreams/microjets can reach 700 m/s. These microstreams/microjets can enhance the permeability of cell membranes due to the formation of transient pores (Fig. 2(b)) [20]. In the presence of nano-/microbubbles, the threshold for cavitation decreases, and it results in rendering their destruction feasible at lower energies of ultrasound.

4. Gene delivery using sonoporation as a non-viral vector system

The first studies investigating the utility of ultrasound for gene delivery used frequencies in the range 20–50 kHz [7,44]. However, these frequencies, along with cavitation, are known to cause tissue damage if not properly controlled [45,46]. To overcome this problem, many gene delivery studies have used therapeutic ultrasound, which operates at frequencies of 1–3 MHz, intensities of 0.5–2.5 W/cm^2 or MI 0.3–2, and in pulse-mode [47]. However, as these conditions result in very inefficient gene delivery, therapeutic ultrasound combined with nano/microbubble contrast agents has been investigated for enhancing gene transfection efficiency [9,13,48,49]. This combination method has many of the characteristics required for practical gene therapy including low toxicity, the potential for repeated applications, organ specificity and broad applicability to acoustically accessible organs. Under proper conditions, the combination of ultrasound and nano/microbubbles can create transient non-lethal perforations in cell membranes. Taniyama et al. reported that transient pores formed in cell membranes upon exposure to ultrasound and Optison, and that the pores completely closed [20]. In addition, the behavior of insonated microbubbles was observed with high-speed camera microscopy [50]. Exposure to high intensity ultrasound induced complete disruption of the microbubbles. The above findings suggest that the combination of microbubbles and ultrasound could be useful for gene delivery (Fig. 2(c)).

4.1. Applying to plasmid DNA delivery

Much research has been conducted both *in vitro* and *in vivo* into gene delivery using ultrasound to disrupt microbubbles. In early feasibility studies, reporter genes such as luciferase, β-galactosidase and green fluorescent protein (GFP) were utilized to assess transfection efficiency [13,51–54]. Transfection method in *in vitro* study is very simple. In general, cells suspended with microbubbles and plasmid DNA were exposed with ultrasound for a few second-several tens of seconds due to be completed transfection in a short period of time [27]. Transfection efficiency is affected by ultrasound exposure condition such as intensity, frequency, period, duty cycle, or type and concentration of microbubble [10,11,13,14]. Normally, the efficiency increase according to increasing ultrasound intensity and period [11]. On the other hand, it was reported that the efficiency and cell viability by the transfection with fractionated exposure was higher than that with continuous exposure in the same period of total exposure [19]. In addition, it was reported that there was optimal concentration of microbubbles [55]. Unfortunately, optimal condition is not completely clear in the transfection using this system because of many changeable parameters as mentioned above. Thus, some researchers have studies the properties of this transfection technology to find out optimal condition.

Many of *in vivo* early studies focused on organs and tissues that are readily imaged by diagnostic ultrasonography, including heart [52,56], skeletal muscle [51] and kidney [57]. Bekeredjian et al. reported the use of ultrasound and microbubbles to deliver reporter genes into heart [56]. Subsequently, Korpanty et al. succeeded in delivering the gene for vascular endothelial growth factor (VEGF) into heart using the same gene delivery system, and VEGF-mediated angiogenesis to rat myocardium [58]. This technique has begun to be broadly utilized as a gene delivery system to other organs, tissues and cells such as the vascular system, pancreas, central nerve system, tumors, and hematopoietic cells. For example, Shimamura et al. reported transfection to the central nervous system by sonoporation after injection of a reporter gene and Optison into cistern magna or striatum [59]. In this study, transfection by microbubbles using ultrasound transferred the reporter gene into cells around the neurons, and not into the neuron cells themselves. Takahashi et al. reported gene transfer into the spine using ultrasound and microbubbles [60]. In addition, Aoi et al. developed herpes simplex virus mediated thymidine kinase (HSV-tk)-mediated suicide gene therapy using nanobubbles and ultrasound [61]. In this therapy, HSV-tk corded plasmid DNA and nanobubbles were injected into tumor tissue of mice, and ultrasound was transdermally exposed toward the tissue. The reduction of tumor size was observed by administration of ganciclovir in the mice transfected HSV-tk corded plasmid DNA with nanobubbles and ultrasound. Previously, we developed novel liposomal nanobubble (Bubble liposome) entrapping perfluoropropane gas (Fig. 3(a–c)) [11,27]. The size of Bubble liposomes was about 500 nm and they were much smaller than Sonazoid (Fig. 3(b)). Bubble liposome could also utilize as an effective plasmid DNA delivery tool *in vitro* (Fig. 3(d)) and *in vivo* by the combination with ultrasound. We reported the utility of Bubble liposome in cancer gene therapy using interleukin-12 (IL-12) corded plasmid DNA [24]. The combination of Bubble liposomes and ultrasound dramatically suppressed tumor growth (Fig. 4). As mentioned above, sonoporation combined with nano/microbubbles could be a good system for plasmid DNA delivery.

4.2. Applying to oligonucleotide delivery

Oligonucleotides such as antisense, decoy and small interfering RNA (siRNA) are important molecules that can stop the expression of specific genes [62,63]. In particular, RNA interference (RNAi) using siRNA has potential in the development of new treatments for disease,

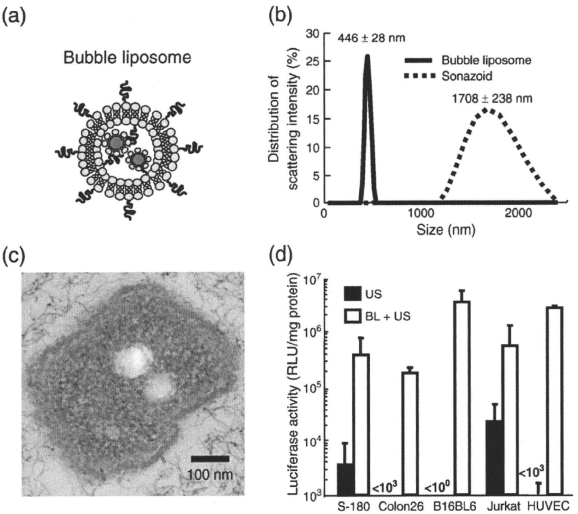

Fig. 3. Comparison of microbubbles and Bubble liposomes (a) Schematic of Bubble liposome. (b) Size distribution of Sonazoid and Bubble liposomes as measured by dynamic light scattering. (c) Transmission electron microscopy (50,000×) of Bubble liposome. (d) Luciferase expression in various types of cells transfected using Bubble liposomes and ultrasound. Cells (1×10^5 cells/500 μL) mixed with pCMV-Luc (5 μg) and Bubble liposomes (60 μg) were exposed or not to ultrasound (frequency, 2 MHz; duty, 50%; burst rate, 2 Hz; intensity, 2.5 W/cm^2; time 10 *s*). The cells were washed and cultured for 2 days. Thereafter, luciferase activity was determined with luminometer. Data are shown as means ± S.D. ($n=3$). BL, Bubble liposome, pCMV-Luc: luciferase corded plasmid DNA, HUVEC: human umbilical vascular endothelial cell.

including malignant, infectious and autoimmune diseases. In order to achieve efficient gene silencing, it is important that the siRNA is introduced into the cytoplasm of the target cell [64]. Diverse approaches have been attempted to develop efficient oligonucleotide delivery methods [62]. However, technologies that enable the tissue-targeted delivery of siRNA using non-viral vectors need improvement.

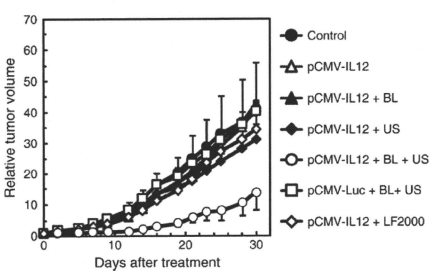

Fig. 4. Cancer gene therapy by IL-12 gene delivery with Bubble liposomes and ultrasound B6C3F1 mice were intradermally inoculated with 1×10^6 OV-HM cells into the flank. On day 7 after tumor inoculation, the tumors were injected with pCMV-IL12 (10 μg) using Bubble liposomes (2.5 μg) and/or ultrasound (1 MHz, 0.7 W/cm^2, 1 min), or Lipofectamine 2000 as a conventional lipofection method. (b) Therapeutic effect was assessed by measuring tumor growth. The volume of the growing tumors was calculated by: (tumor volume; mm^3) = (major axis; mm) × (minor axis; mm)^2 × 0.5). The data are represented as tumor volume relative to the tumor volume on day 7 after tumor inoculation. Each point represents the mean ± SD ($n=5$). BL: Bubble liposomes, US: Ultrasound, LF2000: Lipofectamine 2000, pCMV-IL-12: IL-12 corded plasmid DNA, pCMV-Luc: Luciferase corded plasmid DNA.

As mentioned above, the combination of ultrasound and nano/microbubbles can directly deliver extracellular molecules into the cytosol [25], where antisense, decoy and siRNA function, so this delivery system might better exhibit the functions of these oligonucleotides. Azuma et al. reported that NF-κB decoy delivery into transplanted kidney by the combination of microbubbles and ultrasound could significantly decrease IL-1β and TNF-α (inflammatory cytokines) and prolonged the survival rate of kidney-transplanted mice [57]. Negishi et al. reported that siRNA was directly introduced into the cytoplasm by nanobubbles and ultrasound [30]. In addition, transfection of siRNA into tibialis muscles with nanobubble and ultrasound resulted in gene-silencing, which was sustained for more than 3 weeks. It therefore appears that the combination of nano/microbubbles and ultrasound could be a useful siRNA delivery system. In addition, siRNA transfection with ultrasound and microbubbles was utilized to apply to mesenchymal stem cells, indicating that this technique could be applicable to genetically modified stem cell therapy. Vandenbroucke et al. also developed an interesting siRNA delivery system using sonoporation [65]. They coupled (PEG-siPlex) of PEGylated cationic liposomes and siRNA, and introduced the complex into gas-filled lipid microbubbles. Both the microbubbles and PEG-siPlex, which were modified with biotin, were attached via avidin. Although PEG-siPlex can protect siRNA from digestion by nucleases *in vivo*, PEGylation makes it difficult for the siRNA to be recognized and taken up by the target cells. The microbubble/sonication system should be able to overcome the negative effects of PEGylating siRNA-cationic liposomes (siPlex) and enhance the efficiency of ultrasound-assisted siRNA delivery. Although siRNA delivery mediated by ultrasound and nano/microbubbles must be optimized, this system may open up new perspectives for ultrasound-controlled *in vivo* siRNA delivery.

5. Efforts to tissue- or organ-selective gene delivery

To establish ideal gene therapy, it is important to deliver therapeutic gene into target tissue or organ. In the early study, gene and nano/microbubbles were directly injected into target tissue and organ [53,66]. However, in this method, there are some limitations such as injection volume and injection technique. To improve these problems, some researchers recently developed ultrasound-mediated gene delivery by the supplying gene and nano/microbubbles via blood flow [11,67]. In this delivery, gene expression was limited in the area exposed ultrasound. Ultrasound can be easily focused to a target tissue or organ. Therefore, it might be possible to develop an optimal tissue- or organ-specific gene delivery system by combining nano/microbubble targeting and focused ultrasound. Shen et al. succeeded to developed ultrasound-mediated gene expression in liver via intraportal injection of plasmid DNA and microbubbles [68]. Grayburn et al. reported insulin expression following insulin gene delivery to pancreatic islets in rat by a combination of microbubbles and ultrasound exposure and succeeded to decrease blood glucose level in diabetes rat [67,69]. We also developed the gene delivery into tumor tissue by the combination of injection from tumor dominant artery and ultrasound exposure toward tumor tissue [11]. In addition, transdermal ultrasound exposure toward liver could induce liver selective gene expression after systemic injection of plasmid DNA and Bubble liposomes. In this case, luciferase expression was dominantly observed in the parenchymal cells of liver. These results suggested that Bubble liposomes could quickly transduce plasmid DNA into each tissue by cavitation even under the existence of blood stream. Moreover, we developed the combination method using mannosylated lipoplexes and Bubble liposomes with ultrasound to enhance gene transfection in mannose receptor-expressing cells in liver [29]. In this study, after systemic injection of mannosylated lipoplex, Bubble liposomes were systemically injected and ultrasound was transdermally exposed toward liver. Gene expression was observed mannose receptor-expressing cells such as macrophage and dendritic cells which were known as antigen presenting cells. It is expected that ultrasound-mediated gene delivery with nano/microbubbles might be useful to develop target tissue or organ-selective gene delivery in vivo.

Previously, several groups have reported active targetable nano/microbubbles to endothelium [70], rejected tissues [71], neovasculature endothelium [72], lymph node-related vasculature [73] and activated platelets[74] by targeting ICAM-1 [75], VCAM-1 [76] or integrins [77]. We also developed blood clot targetable Bubble liposomes modified with arginine-glycine-aspartic acid (RGD) peptides to develop effective ultrasound contrast agents for blood clots imaging [78]. Although these nano/microbubbles were developed as ultrasound imaging agents, it might be possible to develop an optimal tissue- or organ-selective gene delivery system by combining targetable nano/microbubble associated with gene and ultrasound.

6. Conclusion

Ultrasound has long been utilized as a useful diagnostic tool. Therapeutic ultrasound was recently developed and is being utilized in clinical settings. The combination of therapeutic ultrasound and nano/microbubbles is an interesting and important system for establishing a novel and non-invasive gene delivery system. Gene expression efficiency with this system can effectively deliver gene compared with conventional non-viral vector system such as lipofection method due to deliver gene into cytosol without endocytosis pathway. Many *in vivo* studies has been reported about ultrasound-mediated gene delivery with nano/microbubbles. Especially, there are some reports about feasibility studies of gene therapy for various diseases [24,29,61,67] In addition, this system has a potency of site specific gene delivery by the control of ultrasound exposure site. Therefore, it is expected that this technology would be utilized as a novel gene delivery system in clinical field.

References

[1] E. Check, Safety panel backs principle of gene-therapy trials, Nature 420 (2002) 595.
[2] E. Check, Second cancer case halts gene-therapy trials, Nature 421 (2003) 305.
[3] E. Marshall, Gene therapy death prompts review of adenovirus vector Science 286 (1999) 2244–2245.
[4] K. Kogure, H. Akita, Y. Yamada, H. Harashima, Multifunctional envelope-type nano device (MEND) as a non-viral gene delivery system, Adv. Drug Deliv. Rev. 60 (2008) 559–571.
[5] F. Liu, C.C. Conwell, X. Yuan, L.M. Shollenberger, L. Huang, Novel nonviral vectors target cellular signaling pathways: regulated gene expression and reduced toxicity, J. Pharmacol. Exp. Ther. 321 (2007) 777–783.
[6] K. Itaka, S. Ohba, K. Miyata, H. Kawaguchi, K. Nakamura, T. Takato, U.I. Chung, K. Kataoka, Bone regeneration by regulated in vivo gene transfer using biocompatible polyplex nanomicelles, Mol. Ther. 15 (2007) 1655–1662.
[7] M. Fechheimer, J.F. Boylan, S. Parker, J.E. Sisken, G.L. Patel, S.G. Zimmer, Transfection of mammalian cells with plasmid DNA by scrape loading and sonication loading, Proc. Natl. Acad. Sci. U. S. A. 84 (1987) 8463–8467.
[8] M.W. Miller, D.L. Miller, A.A. Brayman, A review of in vitro bioeffects of inertial ultrasonic cavitation from a mechanistic perspective, Ultrasound Med. Biol. 22 (1996) 1131–1154.
[9] W.J. Greenleaf, M.E. Bolander, G. Sarkar, M.B. Goldring, J.F. Greenleaf, Artificial cavitation nuclei significantly enhance acoustically induced cell transfection, Ultrasound Med. Biol. 24 (1998) 587–595.
[10] L.B. Feril Jr., R. Ogawa, K. Tachibana, T. Kondo, Optimized ultrasound-mediated gene transfection in cancer cells, Cancer Sci. 97 (2006) 1111–1114.
[11] R. Suzuki, T. Takizawa, Y. Negishi, N. Utoguchi, K. Sawamura, K. Tanaka, E. Namai, Y. Oda, Y. Matsumura, K. Maruyama, Tumor specific ultrasound enhanced gene transfer in vivo with novel liposomal bubbles, J. Control. Release 125 (2008) 137–144.
[12] S.V. Pislaru, C. Pislaru, R.R. Kinnick, R. Singh, R. Gulati, J.F. Greenleaf, R.D. Simari, Optimization of ultrasound-mediated gene transfer: comparison of contrast agents and ultrasound modalities, Eur. Heart J. 24 (2003) 1690–1698.
[13] T. Li, K. Tachibana, M. Kuroki, M. Kuroki, Gene transfer with echo-enhanced contrast agents: comparison between Albunex, Optison, and Levovist in mice–initial results, Radiology 229 (2003) 423–428.
[14] M.A. Hassan, M.A. Buldakov, R. Ogawa, Q.L. Zhao, Y. Furusawa, N. Kudo, T. Kondo, P. Riesz, Modulation control over ultrasound-mediated gene delivery: evaluating the importance of standing waves, J. Control. Release 141 (2010) 70–76.
[15] D.J. Wells, Electroporation and ultrasound enhanced non-viral gene delivery in vitro and in vivo, Cell Biol. Toxicol. 26 (2010) 21–28.
[16] M.A. Hassan, L.B. Feril Jr., K. Suzuki, N. Kudo, K. Tachibana, T. Kondo, Evaluation and comparison of three novel microbubbles: enhancement of ultrasound-induced cell death and free radicals production, Ultrason. Sonochem. 16 (2009) 372–378.
[17] L.B. Feril Jr., T. Kondo, Q.L. Zhao, R. Ogawa, K. Tachibana, N. Kudo, S. Fujimoto, S. Nakamura, Enhancement of ultrasound-induced apoptosis and cell lysis by echo-contrast agents, Ultrasound Med. Biol. 29 (2003) 331–337.
[18] N. Kudo, K. Okada, K. Yamamoto, Sonoporation by single-shot pulsed ultrasound with microbubbles adjacent to cells, Biophys. J. 96 (2009) 4866–4876.
[19] D.P. Guo, X.Y. Li, P. Sun, Y.B. Tang, X.Y. Chen, Q. Chen, L.M. Fan, B. Zang, L.Z. Shao, X.R. Li, Ultrasound-targeted microbubble destruction improves the low density lipoprotein receptor gene expression in HepG2 cells, Biochem. Biophys. Res. Commun. 343 (2006) 470–474.
[20] Y. Taniyama, K. Tachibana, K. Hiraoka, T. Namba, K. Yamasaki, N. Hashiya, M. Aoki, T. Ogihara, K. Yasufumi, R. Morishita, Local delivery of plasmid DNA into rat carotid artery using ultrasound, Circulation 105 (2002) 1233–1239.
[21] Z. Gao, A.M. Kennedy, D.A. Christensen, N.Y. Rapoport, Drug-loaded nano/microbubbles for combining ultrasonography and targeted chemotherapy, Ultrasonics 48 (2008) 260–270.
[22] Y. Wang, X. Li, Y. Zhou, P. Huang, Y. Xu, Preparation of nanobubbles for ultrasound imaging and intracelluar drug delivery, Int. J. Pharm. 384 (2010) 148–153.
[23] R. Suzuki, K. Maruyama, Effective in vitro and in vivo gene delivery by the combination of liposomal bubbles (bubble liposomes) and ultrasound exposure, Methods Mol. Biol. 605 (2009) 473–486.
[24] R. Suzuki, E. Namai, Y. Oda, N. Nishiie, S. Otake, R. Koshima, K. Hirata, Y. Taira, N. Utoguchi, Y. Negishi, S. Nakagawa, K. Maruyama, Cancer gene therapy by IL-12 gene delivery using liposomal bubbles and tumoral ultrasound exposure, J. Control. Release 142 (2010) 245–250.
[25] R. Suzuki, Y. Oda, N. Utoguchi, E. Namai, Y. Taira, N. Okada, N. Kadowaki, T. Kodama, K. Tachibana, K. Maruyama, A novel strategy utilizing ultrasound for antigen delivery in dendritic cell-based cancer immunotherapy, J. Control. Release 133 (2009) 198–205.
[26] R. Suzuki, T. Takizawa, Y. Kuwata, M. Mutoh, N. Ishiguro, N. Utoguchi, A. Shinohara, M. Eriguchi, H. Yanagie, K. Maruyama, Effective anti-tumor activity of oxaliplatin encapsulated in transferrin-PEG-liposome, Int. J. Pharm. 346 (2008) 143–150.
[27] R. Suzuki, T. Takizawa, Y. Negishi, K. Hagisawa, K. Tanaka, K. Sawamura, N. Utoguchi, T. Nishioka, K. Maruyama, Gene delivery by combination of novel liposomal bubbles with perfluoropropane and ultrasound, J. Control. Release 117 (2007) 130–136.
[28] R. Suzuki, T. Takizawa, Y. Negishi, N. Utoguchi, K. Maruyama, Effective gene delivery with liposomal bubbles and ultrasound as novel non-viral system, J. Drug Target. 15 (2007) 531–537.

[29] K. Un, S. Kawakami, R. Suzuki, K. Maruyama, F. Yamashita, M. Hashida, Enhanced transfection efficiency into macrophages and dendritic cells by a combination method using mannosylated lipoplexes and bubble liposomes with ultrasound exposure, Hum. Gene Ther. 21 (2010) 65–74.
[30] Y. Negishi, Y. Endo, T. Fukuyama, R. Suzuki, T. Takizawa, D. Omata, K. Maruyama, Y. Aramaki, Delivery of siRNA into the cytoplasm by liposomal bubbles and ultrasound, J. Control. Release 132 (2008) 124–130.
[31] Y. Negishi, D. Omata, H. Iijima, Y. Takabayashi, K. Suzuki, Y. Endo, R. Suzuki, K. Maruyama, M. Nomizu, Y. Aramaki, Enhanced laminin-derived peptide AG73-mediated liposomal gene transfer by bubble liposomes and ultrasound, Mol. Pharm. 7 (2010) 217–226.
[32] T. Yamashita, S. Sonoda, R. Suzuki, N. Arimura, K. Tachibana, K. Maruyama, T. Sakamoto, A novel bubble liposome and ultrasound-mediated gene transfer to ocular surface: RC-1 cells in vitro and conjunctiva in vivo, Exp. Eye Res . 85 (2007) 741–748.
[33] P.M. Shah, R. Gramiak, D.H. Kramer, P.N. Yu, Determinants of atrial (S4) and ventricular (S3) gallop sounds in primary myocardial disease, N Engl J. Med. 278 (1968) 753–758.
[34] A. Kabalnov, D. Klein, T. Pelura, E. Schutt, J. Weers, Dissolution of multicomponent microbubbles in the bloodstream: 1, Theory Ultrasound Med Biol 24 (1998) 739–749.
[35] K. Yanagisawa, F. Moriyasu, T. Miyahara, M. Yuki, H. Iijima, Phagocytosis of ultrasound contrast agent microbubbles by Kupffer cells, Ultrasound Med. Biol. 33 (2007) 318–325.
[36] R. Watanabe, M. Matsumura, T. Munemasa, M. Fujimaki, M. Suematsu, Mechanism of hepatic parenchyma-specific contrast of microbubble-based contrast agent for ultrasonography: microscopic studies in rat liver, Invest. Radiol. 42 (2007) 643–651.
[37] K. Korenaga, M. Korenaga, M. Furukawa, T. Yamasaki, I. Sakaida, Usefulness of Sonazoid contrast-enhanced ultrasonography for hepatocellular carcinoma: comparison with pathological diagnosis and superparamagnetic iron oxide magnetic resonance images, J. Gastroenterol. 44 (2009) 733–741.
[38] E.C. Unger, E. Hersh, M. Vannan, T.O. Matsunaga, T. McCreery, Local drug and gene delivery through microbubbles, Prog. Cardiovasc. Dis. 44 (2001) 45–54.
[39] S.L. Mulvagh, A.N. DeMaria, S.B. Feinstein, P.N. Burns, S. Kaul, J.G. Miller, M. Monaghan, T.R. Porter, L.J. Shaw, F.S. Villanueva, Contrast echocardiography: current and future applications, J. Am. Soc. Echocardiogr. 13 (2000) 331–342.
[40] A. van Wamel, K. Kooiman, M. Harteveld, M. Emmer, F.J. ten Cate, M. Versluis, N. de Jong, Vibrating microbubbles poking individual cells: drug transfer into cells via sonoporation, J. Control. Release 112 (2006) 149–155.
[41] M. Duvshani-Eshet, L. Baruch, E. Kesselman, E. Shimoni, M. Machluf, Therapeutic ultrasound-mediated DNA to cell and nucleus: bioeffects revealed by confocal and atomic force microscopy, Gene Ther. 13 (2006) 163–172.
[42] M. Duvshani-Eshet, D. Adam, M. Machluf, The effects of albumin-coated microbubbles in DNA delivery mediated by therapeutic ultrasound, J. Control. Release 112 (2006) 156–166.
[43] K. Kalantarinia, J.T. Belcik, J.T. Patrie, K. Wei, Real-time measurement of renal blood flow in healthy subjects using contrast-enhanced ultrasound, Am. J. Physiol. Ren. Physiol 297 (2009) F1129–F1134.
[44] M. Joersbo, J. Brunstedt, Protein synthesis stimulated in sonicated sugar beet cells and protoplasts, Ultrasound Med. Biol. 16 (1990) 719–724.
[45] H.R. Guzman, A.J. McNamara, D.X. Nguyen, M.R. Prausnitz, Bioeffects caused by changes in acoustic cavitation bubble density and cell concentration: a unified explanation based on cell-to-bubble ratio and blast radius, Ultrasound Med. Biol. 29 (2003) 1211–1222.
[46] W. Wei, B. Zheng-zhong, W. Yong-jie, Z. Qing-wu, M. Ya-lin, Bioeffects of low-frequency ultrasonic gene delivery and safety on cell membrane permeability control, J. Ultrasound Med. 23 (2004) 1569–1582.
[47] H.J. Kim, J.F. Greenleaf, R.R. Kinnick, J.T. Bronk, M.E. Bolander, Ultrasound-mediated transfection of mammalian cells, Hum. Gene Ther. 7 (1996) 1339–1346.
[48] D.M. Hallow, A.D. Mahajan, T.E. McCutchen, M.R. Prausnitz, Measurement and correlation of acoustic cavitation with cellular bioeffects, Ultrasound Med. Biol. 32 (2006) 1111–1122.
[49] R.V. Shohet, S. Chen, Y.T. Zhou, Z. Wang, R.S. Meidell, R.H. Unger, P.A. Grayburn, Echocardiographic destruction of albumin microbubbles directs gene delivery to the myocardium, Circulation 101 (2000) 2554–2556.
[50] A. van Wamel, A. Bouakaz, M. Versluis, N. de Jong, Micromanipulation of endothelial cells: ultrasound-microbubble-cell interaction, Ultrasound Med. Biol. 30 (2004) 1255–1258.
[51] J.P. Christiansen, B.A. French, A.L. Klibanov, S. Kaul, J.R. Lindner, Targeted tissue transfection with ultrasound destruction of plasmid-bearing cationic microbubbles, Ultrasound Med. Biol. 29 (2003) 1759–1767.
[52] S. Chen, R.V. Shohet, R. Bekeredjian, P. Frenkel, P.A. Grayburn, Optimization of ultrasound parameters for cardiac gene delivery of adenoviral or plasmid deoxyribonucleic acid by ultrasound-targeted microbubble destruction, J. Am. Coll. Cardiol. 42 (2003) 301–308.
[53] Q.L. Lu, H.D. Liang, T. Partridge, M.J. Blomley, Microbubble ultrasound improves the efficiency of gene transduction in skeletal muscle in vivo with reduced tissue damage, Gene Ther. 10 (2003) 396–405.
[54] S. Tsunoda, O. Mazda, Y. Oda, Y. Iida, S. Akabame, T. Kishida, M. Shin-Ya, H. Asada, S. Gojo, J. Imanishi, H. Matsubara, T. Yoshikawa, Sonoporation using microbubble BR14 promotes pDNA/siRNA transduction to murine heart, Biochem. Biophys. Res. Commun. 336 (2005) 118–127.
[55] Y. Taniyama, K. Tachibana, K. Hiraoka, M. Aoki, S. Yamamoto, K. Matsumoto, T. Nakamura, T. Ogihara, Y. Kaneda, R. Morishita, Development of safe and efficient novel nonviral gene transfer using ultrasound: enhancement of transfection efficiency of naked plasmid DNA in skeletal muscle, Gene Ther. 9 (2002) 372–380.
[56] R. Bekeredjian, S. Chen, P.A. Frenkel, P.A. Grayburn, R.V. Shohet, Ultrasound-targeted microbubble destruction can repeatedly direct highly specific plasmid expression to the heart, Circulation 108 (2003) 1022–1026.
[57] H. Azuma, N. Tomita, Y. Kaneda, H. Koike, T. Ogihara, Y. Katsuoka, R. Morishita, Transfection of NFkappaB-decoy oligodeoxynucleotides using efficient ultrasound-mediated gene transfer into donor kidneys prolonged survival of rat renal allografts, Gene Ther. 10 (2003) 415–425.
[58] G. Korpanty, S. Chen, R.V. Shohet, J. Ding, B. Yang, P.A. Frenkel, P.A. Grayburn, Targeting of VEGF-mediated angiogenesis to rat myocardium using ultrasonic destruction of microbubbles, Gene Ther. 12 (2005) 1305–1312.
[59] M. Shimamura, N. Sato, Y. Taniyama, S. Yamamoto, M. Endoh, H. Kurinami, M. Aoki, T. Ogihara, Y. Kaneda, R. Morishita, Development of efficient plasmid DNA transfer into adult rat central nervous system using microbubble-enhanced ultrasound, Gene Ther. 11 (2004) 1532–1539.
[60] M. Takahashi, K. Kido, A. Aoi, H. Furukawa, M. Ono, T. Kodama, Spinal gene transfer using ultrasound and microbubbles, J. Control. Release 117 (2007) 267–272.
[61] A. Aoi, Y. Watanabe, S. Mori, M. Takahashi, G. Vassaux, T. Kodama, Herpes simplex virus thymidine kinase-mediated suicide gene therapy using nano/microbubbles and ultrasound, Ultrasound Med. Biol. 34 (2008) 425–434.
[62] E. Fattal, G. Barratt, Nanotechnologies and controlled release systems for the delivery of antisense oligonucleotides and small interfering RNA, Br. J. Pharmacol. 157 (2009) 179–194.
[63] S. Kimura, K. Egashira, L. Chen, K. Nakano, E. Iwata, M. Miyagawa, H. Tsujimoto, K. Hara, R. Morishita, K. Sueishi, R. Tominaga, K. Sunagawa, Nanoparticle-mediated delivery of nuclear factor kappaB decoy into lungs ameliorates monocrotaline-induced pulmonary arterial hypertension, Hypertension 53 (2009) 877–883.
[64] K. Tiemann, J.J. Rossi, RNAi-based therapeutics-current status, challenges and prospects EMBO, Mol. Med. 1 (2009) 142–151.
[65] R.E. Vandenbroucke, I. Lentacker, J. Demeester, S.C. De Smedt, N.N. Sanders, Ultrasound assisted siRNA delivery using PEG-siPlex loaded microbubbles, J. Control. Release 126 (2008) 265–273.
[66] C.H. Miao, A.A. Brayman, K.R. Loeb, P. Ye, L. Zhou, P. Mourad, L.A. Crum, Ultrasound enhances gene delivery of human factor IX plasmid, Hum. Gene Ther. 16 (2005) 893–905.
[67] S. Chen, J.H. Ding, R. Bekeredjian, B.Z. Yang, R.V. Shohet, S.A. Johnston, H.E. Hohmeier, C.B. Newgard, P.A. Grayburn, Efficient gene delivery to pancreatic islets with ultrasonic microbubble destruction technology, Proc. Natl. Acad. Sci. U. S. A. 103 (2006) 8469–8474.
[68] Z.P. Shen, A.A. Brayman, L. Chen, C.H. Miao, Ultrasound with microbubbles enhances gene expression of plasmid DNA in the liver via intraportal delivery, Gene Ther. 15 (2008) 1147–1155.
[69] R. Chai, S. Chen, J. Ding, P.A. Grayburn, Efficient, glucose responsive and islet-specific transgene expression by a modified rat insulin promoter, Gene Ther. 16 (2009) 1202–1209.
[70] F.S. Villanueva, R.J. Jankowski, S. Klibanov, M.L. Pina, S.M. Alber, S.C. Watkins, G.H. Brandenburger, W.R. Wagner, Microbubbles targeted to intercellular adhesion molecule-1 bind to activated coronary artery endothelial cells, Circulation 98 (1998) 1–5.
[71] G.E. Weller, E. Lu, M.M. Csikari, A.L. Klibanov, D. Fischer, W.R. Wagner, F.S. Villanueva, Ultrasound imaging of acute cardiac transplant rejection with microbubbles targeted to intercellular adhesion molecule-1, Circulation 108 (2003) 218–224.
[72] D.B. Ellegala, H. Leong-Poi, J.E. Carpenter, A.L. Klibanov, S. Kaul, M.E. Shaffrey, J. Sklenar, J.R. Lindner, Imaging tumor angiogenesis with contrast ultrasound and microbubbles targeted to alpha(v)beta3, Circulation 108 (2003) 336–341.
[73] P. Hauff, M. Reinhardt, A. Briel, N. Debus, M. Schirner, Molecular targeting of lymph nodes with L-selectin ligand-specific US contrast agent: a feasibility study in mice and dogs, Radiology 231 (2004) 667–673.
[74] P.A. Schumann, J.P. Christiansen, R.M. Quigley, T.P. McCreery, R.H. Sweitzer, E.C. Unger, J.R. Lindner, T.O. Matsunaga, Targeted-microbubble binding selectively to GPIIb IIIa receptors of platelet thrombi, Invest. Radiol. 37 (2002) 587–593.
[75] G.E. Weller, F.S. Villanueva, E.M. Tom, W.R. Wagner, Targeted ultrasound contrast agents: in vitro assessment of endothelial dysfunction and multi-targeting to ICAM-1 and sialyl Lewisx, Biotechnol. Bioeng. 92 (2005) 780–788.
[76] C.Z. Behm, B.A. Kaufmann, C. Carr, M. Lankford, J.M. Sanders, C.E. Rose, S. Kaul, J.R. Lindner, Molecular imaging of endothelial vascular cell adhesion molecule-1 expression and inflammatory cell recruitment during vasculogenesis and ischemia-mediated arteriogenesis, Circulation 117 (2008) 2902–2911.
[77] J.R. Lindner, Detection of inflamed plaques with contrast ultrasound, Am. J. Cardiol. 90 (2002) 32L–35L.
[78] K. Hagisawa, N.T., K. Iida, H. Luo, R.J. Siegel, Thrombolysis using low frequency ultrasound with activated platelet targeting bubble liposome in a rabbit iliac artery, Circulation 112 (Sup.II) (2005) 503.

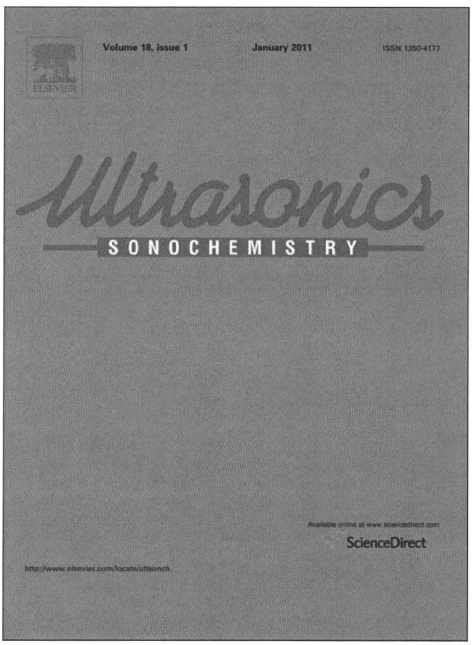

Ultrasonics Sonochemistry 18 (2011) 425–430

Contents lists available at ScienceDirect

Ultrasonics Sonochemistry

journal homepage: www.elsevier.com/locate/ultsonch

Synergistic effect of ultrasound and antibiotics against *Chlamydia trachomatis*-infected human epithelial cells in vitro

Yurika Ikeda-Dantsuji [a], Loreto B. Feril Jr. [a,*], Katsuro Tachibana [a], Koichi Ogawa [a], Hitomi Endo [a], Yoshimi Harada [a], Ryo Suzuki [b], Kazuo Maruyama [b]

[a] Department of Anatomy, Fukuoka University School of Medicine, Fukuoka, Japan
[b] Department of Biopharmaceutics, School of Pharmaceutical Sciences, Teikyo University, Kanagawa, Japan

ARTICLE INFO

Article history:
Received 12 April 2010
Received in revised form 12 July 2010
Accepted 21 July 2010
Available online 27 July 2010

Keywords:
Ultrasound
Nanobubbles
Antibiotic
Intracellular bacteria

ABSTRACT

To investigate whether or not the combined ultrasound and antibiotic treatment is effective against chlamydial infection, a new ultrasound exposure system was designed to treat chlamydia-infected cells. First, the minimum inhibitory concentrations of antibiotics against *Chlamydia trachomatis* were determined. Infected cultures were treated with antibiotics then sonicated at intensity of 0.15 or 0.44 W/cm^2 with or without Bubble liposomes. After 48 or 72 h after infection, chlamydial inclusions were stained and examined by fluorescence microscopy. The internalization of dextran–fluorescein conjugates by ultrasound irradiation with Bubble liposomes was observed by fluorescence microscopy. The results showed that application of nanobubble-enhanced ultrasound caused no significant effect on cell viability and chlamydial infectivity. However, Doxycycline (1/2 MIC) or CZX (1.0 μg/ml) in combination with nanobubble-enhanced ultrasound dramatically reduced the number of inclusions compared with that administered with antibiotics only. Bubble dose-dependent synergy was also observed. After ultrasound irradiation at intensity of 0.44 W/cm^2 on the presence of Bubble liposomes, 10% of HeLa cells were observed to have internalized the dextran molecules. This study suggests the possibility of using nanobubble-enhanced ultrasound to deliver antibiotic molecules into cells to eradiate intracellular bacteria, such as chlamydiae, without causing much damage to the cells itself.

1. Introduction

An obligate intracellular pathogen, *Chlamydia trachomatis*, is the most prevalent sexually transmitted bacterium worldwide [1]. *C. trachomatis* is a Gram-negative bacterium which has a unique biphasic developmental cycle characterized by an infectious but metabolically inactive extracellular form, called the 'elementary body', which initiates infection through the uptake by the host cell. Thereafter, elementary bodies differentiate into noninfectious but metabolically active forms, called the 'reticulate body', which proliferate within the inclusion. Reticulate bodies also differentiate back to elementary bodies before release at the end of the developmental cycle. At its sites of primary infection, *C. trachomatis* infects the urethral or cervical epithelium, causing acute urethritis or cervicitis [2]. These frequently progress into chronic inflammatory disease, the most significant of which, is chronic salpingitis, an inflammatory disease of fallopian tubes that can result in pelvic inflammatory disease, ectopic pregnancy, and tubal infertility [3].

The recommended antibiotic treatments for urogenital infections are a single dose of azithromycin or a 7-day course of doxycycline for management of active infections [4]. These regimens have been shown to result in satisfactory cure rates of acute infections [5,6]; however, chronic diseases (designated "persistent infection") have been suggested to be less responsive to antibiotic therapy [7].

Previous work has shown that some antibiotics treatment of *Pseudomonas aeruginosa* or *Escherichia coli* coupled with ultrasound irradiation enhances the bactericidal activity [8]. The more recent research has revealed that similar synergistic effects of combined ultrasound and antibiotic treatment are seen in both Gram-positive and Gram-negative bacteria with some antibiotics, especially the aminoglycosides [9]. It is not clear whether the combined ultrasound and antibiotic treatment are effective on intracellular pathogen, e.g. chlamydial infection. If an intracellular bacterial infection could be efficiently eradicated from an infected person, one could avoid chronic antibiotic treatments. In addition, this strategy of treatment could be beneficial in the management of chlamydial persistent diseases.

Here, we are studying the synergistic use of ultrasound and antibiotics to kill the *chlamydia*. This report presents results of

* Corresponding author. Address: 7-45-1 Nanakuma, Jonan-ku, Fukuoka 814-0180 Japan. Tel.: +81 92 801 1011x3206; fax: +81 92 865 6032.
E-mail addresses: ferilism@yahoo.com, feril@fukuoka-u.ac.jp (LB. Feril).

1350-4177/$ - see front matter © 2010 Elsevier B.V. All rights reserved.
doi:10.1016/j.ultsonch.2010.07.015

the first step in that research, which is investigation of the in vitro response of *C. trachomatis*-infected human epithelial cells to combination of ultrasound and two types of antibiotics.

2. Materials and methods

2.1. Chlamydial strain and cell lines

C. trachomatis serovar E/UW-5/Cx was prepared in McCoy cells and propagated according to a previously reported method [10]. The mouse fibroblast cell line McCoy cell (CRL 1696) and human epithelial cell line HeLa 229 cell (CLL 2.1) were maintained in Dulbecco's modified Eagle medium (DMEM, Invitrogen, Grand Island, NY, USA) supplemented with 10% heat-inactivated fetal calf serum (FCS, Invitrogen) and 100 μg/ml streptomycin.

2.2. Infection of HeLa cells

The HeLa cells were seeded into a 24-well plate with lumox™ fluorocarbon film base (optically clear, 50 μm-thin, gas permeable film, Greiner bio-one, Gottingen, Germany). Stocks of chlamydial strain were diluted with sucrose–phosphate–glutamate (SPG) medium [10]. Chlamydial suspensions of 0.5×10^4 inclusion-forming units (IFUs) in 0.25 ml SPG medium were inoculated onto the monolayer cultures of HeLa cells (1×10^4 cells/well). This is equivalent to a multiplicity of infection of 0.5. After incubation at 37 °C for 90 min, the inoculum was decanted, and the cells were washed in medium to remove the nonadsorbed chlamydiae and were then further incubated in 1 ml DMEM containing 1 μg/ml cycloheximide (Sigma Chemicals, St. Louis, MO, USA) and 2% FCS (maintenance medium).

2.3. Preparation of bubble liposome

Bubble liposomes were prepared according to a method previously described [11]. Liposomes composed of 1,2-distearoyl-sn-glycero-phosphatidylcholine (DSPC) (NOF Corp., Tokyo, Japan) and 1,2-distearoyl-snglycero-3-phosphatidyl-ethanolamine-methoxypolyethyleneglycol(DSPE-PEG(2k)-OMe, (PEG Mw = ca. 2000), NOF) (94: 6 (m/m)) were prepared by reverse phase evaporation. Briefly, all reagents (totallipid: 100 μmol) were dissolved in 8 ml of 1:1 (v/v) chloroform/diisopropyl ether, then 4 ml of phosphate buffered saline (PBS) were added. The mixture was sonicated and evaporated at 65 °C. The solvent was completely removed, and the size of the liposomes was adjusted to less than 200 nm using an extruding apparatus (Northern Lipids Inc., Vancouver, BC, Canada) and sizing filters (pore sizes: 100 and 200 nm; Nuclepore Track-Etch Membrane, Whatman plc, UK). After sizing, the liposomes were sterilized by passing them through a 0.45 μm pore size filter (MILLEX HV filter unit, Durapore PVDF membrane, Millipore Corp., MA, USA). The size of the liposomes was measured by dynamic light scattering (ELS-800, Otsuka Electronics Co., Ltd., Osaka, Japan). The average diameter of these liposomes was between 150 and 200 nm. Lipid concentration was measured using the Phospholipid C test (Wako Pure Chemical Industries). BLs were prepared from the liposomes and perfluoropropane gas (Takachiho Chemical Industrial Co., Ltd., Tokyo, Japan). Briefly, 5 ml sterilized vials containing 2 ml of the liposome suspension (lipid concentration: 2 mg/ml) were filled with perfluoropropane, capped, and then supercharged with 7.5 ml of perfluoropropane. The vial was placed in a bath-type sonicator (42 kHz, 100 W; BRANSONIC 2510J-DTH, Branson Ultrasonics Co., Danbury, CT, USA) for 5 min to form the BLs. In this method, the liposomes were reconstituted by sonication under the condition of supercharge with perfluoropropane in the 5 ml vial container. At the same time, perfluoropropane would be entrapped within lipids like micelles, which were made by DSPC and DSPE-PEG(2k)-OMe from liposome composition, to form nanobubbles. The lipid nanobubbles were encapsulated within the reconstituted liposomes, which sizes were changed into around 1 μm from 150 to 200 nm of original.

2.4. Immunofluorescence staining and fluorescence microscopy

At 48 or 72 h after infection, the infected monolayers were washed with PBS, and the cells were fixed with −20 °C chilled methanol. After the specimens had been dried, the inclusion bodies were stained with fluorescein isothiocyanate (FITC)-labeled monoclonal antibody against *C. trachomatis* lipopolysaccharides (Progen Biotechnik, Heidelberg, Germany) for 30 min at room temperature. The cells were rinsed with saline, and the films were cut off from the plate, and mounted in a 1:1 solution of PBS–glycerol. The antibody staining resulted in yellow–green chlamydial proteins, and Evans blue counterstaining yielded red eukaryotic cells. The formation of inclusions was assessed using a Zeiss Axiophot fluorescence microscope. The cells positive for inclusions are considered infected cells and infectivity was presented as the number of inclusion-forming units (IFUs).

2.5. Antibiotics and measurements of MICs

Doxycycline (DOX, Sigma Chemicals) and ceftizoxime (CZX, Fujisawa Yakuhin Kogyou, Tokyo, Japan) were obtained in powder form. Both antibiotics were diluted with saline, and were dissolved in maintenance medium at a concentration of 100 μg/ml and frozen at −80 °C until used. The minimum inhibitory concentrations (MICs) were determined using a method previously described [12]. Briefly, confluent monolayer cultures of cells in a 24-well flat-bottomed plate with 13-mm coverslips were inoculated by centrifugation and incubated in 1 ml of maintenance medium containing a serial dilution of antibiotics for 72 h. To determine the MICs, the cover slips were stained and observed as described in Immunofluorescence staining and fluorescence microscopy. The lowest concentration of the antimicrobial agent that completely inhibited the formation of visible chlamydial inclusions was determined as the MIC.

2.6. Ultrasound exposure

An acoustically transparent gel (Pharmaceutical Innovations Inc., Newark, NJ) was applied on the ultrasound probe before positioning the plate containing the sample on top of it (Fig. 1). Thera-

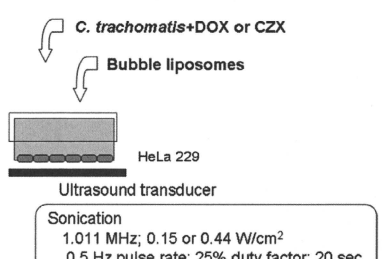

Fig. 1. Experimental design. Schematic drawing of the ultrasound setting. *C. trachomatis*-infected HeLa cells were exposed to ultrasound after addition of antibiotic and Bubble liposomes.